

Mobility and Blockage-aware Communications in Millimeter-Wave Vehicular Networks

Muddassar Hussain[†], Maria Scalabrin[‡], Michele Rossi[‡], and Nicolò Michelusi[†]

Abstract—Mobility may degrade the performance of next-generation vehicular networks operating at the millimeter-wave spectrum: frequent loss of alignment and blockages require repeated beam training and handover, thus incurring huge overhead. In this paper, an adaptive and joint design of beam training, data transmission and handover is proposed, that exploits the mobility process of mobile users (MUs) and the dynamics of blockages to optimally trade-off throughput and power consumption. At each time slot, the serving base station decides to perform either beam training, data communication, or handover when blockage is detected. The decision problem is cast as a partially observable Markov decision process, and the goal is to maximize the throughput delivered to the MU, subject to an average power constraint. To address the high dimensionality of the problem, an approximate dynamic programming algorithm based on a variant of PERSEUS [2] is developed, where both the primal and dual functions are simultaneously optimized to meet the power constraint. Numerical results show that the PERSEUS-based policy has near-optimal performance, and achieves a 55% gain in spectral efficiency compared to a baseline scheme with periodic beam training. Motivated by the structure of the PERSEUS-based policy, two heuristic policies with lower computational cost are proposed. These are shown to achieve a performance comparable to that of PERSEUS, with just a 10% loss in spectral efficiency.

I. INTRODUCTION

Current sub-6GHz vehicular communication systems cannot support the demand of future applications such as autonomous driving, augmented reality and infotainment, due to limited bandwidth availability [3]. To support this demand, new solutions are being explored that leverage the huge amount of bandwidth in the 30 – 300 GHz band, the so called millimeter-wave (mm-wave) spectrum. While communication at these frequencies is ideal to support high capacity demands, it relies on highly directional transmissions and it is susceptible to blockages and mis-alignment, which are exacerbated in highly mobile environments. In this paper, we show that knowledge of the mobility process of mobile users and of blockage dynamics are extremely important in the design of communication strategies: the faster the environment we operate in, the more frequent the loss of alignment and blockages, and the more resources need to be allocated to maintain beam alignment and perform handover to compensate for blockage. However, two key questions arise: *How do we leverage the system dynamics to optimize the communication performance? How much do we gain by doing so?* To address these questions, in this paper we envision the use of adaptive communication strategies and their formulation via partially observable (PO) Markov decision processes (MDPs).

In the proposed scenario, two base stations (BSs) on both sides of a road link serve a mobile user (MU) moving along it. At any time, the MU is associated with one of the two BSs

(the serving BS). To estimate the position of the MU within the road link and enable directional data transmission (DT), the serving BS performs beam training (BT); to compensate for blockage, it performs handover (HO) of the data traffic to the other BS on the opposite side of the road link. The goal is to design the BT/DT/HO strategy so as to maximize the throughput delivered to the MU, subject to an average power constraint. We formulate the optimization problem as a POMDP, and develop an approximate dynamic programming algorithm based on PERSEUS [2]. To meet the average power constraint requirement, we design a variant of PERSEUS which simultaneously optimizes the primal and dual functions, and demonstrate its convergence numerically. Our numerical evaluations based on a data-driven mobility model demonstrate that the PERSEUS-based policy performs very closely to a genie-aided upper bound in which the position of the MU and the blockage states are known, and outperforms a baseline scheme with periodic beam training by up to 55% in spectral efficiency. Motivated by its structure, we design two heuristic policies with lower computational cost – belief-based and finite-state-machine-based heuristics – and show numerically that they incur a small 10% degradation in spectral efficiency compared to PERSEUS-based.

Related Work: Beam training design for mm-wave systems has been an area of extensive research for the past decade, with various approaches proposed, such as beam sweeping [4], estimation of angles of arrival (AoA) and of departure (AoD) [5], and data-assisted schemes [6]. Despite their simplicity, the overhead of these algorithms may ultimately offset the benefits of beamforming in highly mobile environments [3]. While wider beams require less beam training, they result in a lower beamforming gain, hence smaller achievable capacity [7]. While contextual information, such as GPS readings of vehicles [6], may alleviate this overhead, it does not eliminate the need for beam training due to noise and inaccuracies in GPS acquisition. Thus, the design of schemes that alleviate the beam training overhead is of great importance.

In most of the aforementioned works, a priori information on the vehicle’s mobility as well as blockage dynamics is not leveraged in the design of BT/DT protocols. In contrast, we contend that leveraging such information via adaptive communications can greatly improve the performance of automotive networks [8]. In our previous work [9], we bridge this gap by designing adaptive strategies for BT/DT that leverage a priori mobility information via POMDPs, but with no consideration of blockage (hence no handover). Compared to [4], which is based on a “worst-case” mobility pattern, in our previous work [9] we assume a statistical mobility model, where the position of the MU evolves following Markovian dynamics, and exploit these dynamics via POMDPs.

A distinctive feature of the mm-wave channel is its highly dynamic behavior, due to the occurrence of blockages on a very short time scale [10]. In this respect, cell selection repre-

Part of this work has been submitted to IEEE ICC 2020 [1].

[‡]School of Electrical and Computer Engineering, Purdue University, email: {hussai13,michelusi}@purdue.edu

[†]Dept. of Information Engineering, University of Padova, email: {scalabri,rossi}@dei.unipd.it

This research has been funded in part by NSF under grant CNS-1642982.

sents a fundamental functionality to preserve communication in the event of link obstruction: to this end, the quality of the mm-wave link needs to be tightly tracked, and the MU should rapidly switch to another BS in response to the fast-varying link state. Several MDP-based handoff strategies have been investigated over the past decade to solve this problem in the $< 5\text{GHz}$ range [11], [12], as MDPs naturally allow to capture dynamics in the link state. However, these techniques cannot be readily applied to the mm-wave frequencies, which exhibit peculiar features such as fast-varying blockage dynamics. In this paper, we develop techniques to quickly detect blockages and restore beam-alignment via handover.

Related work that applies machine learning to mm-wave networks includes [13]–[17], revealing a growing interest in the design of schemes that exploit side information to enhance the overall network performance. For example, a coordinated beamforming technique using a combination of deep learning and ray-tracing is proposed in [13], demonstrating its ability to efficiently adapt to changing environments. More recent solutions are based on multi-armed bandit, by leveraging *contextual information* to reduce the training overhead as in [14], or the beam alignment feedback to improve the beam search in the next rounds as in [15]–[17]. However, no handover strategies are considered in these works, resulting in limited ability to combat blockage. In addition, these works neglect the impact of realistic mobility and blockage processes on the performance. Compared to this line of works, in this paper, we design adaptive communication strategies that leverage statistical information on the mobility and blockage processes in the selection of BT/DT/HO actions, with the goal to optimize the average long-term communication performance of the system. This approach is in contrast to strategies that either use non-adaptive algorithms [13], lack a mechanism to perform handover [14]–[17], or assume a non realistic mobility pattern in their design.

Our Contributions:

- 1) We define a POMDP framework to optimize the BT/DT/HO strategy in a mm-wave vehicular network, subject to mobility of the MU and time-varying blockage; based on this POMDP formulation, we formulate an optimization problem with the goal to maximize throughput subject to an average power constraint;
- 2) We propose a novel feedback mechanism for BT, which reports the ID of the strongest beam if the received power is above a threshold (a design parameter), otherwise it reports \emptyset to indicate mis-alignment or blockage. We analyze in closed form the feedback distribution and the probability of incorrect detection;
- 3) To address the complexity of POMDPs, we use PERSEUS [2], an approximate point-based value iteration (PBVI) algorithm which optimizes the value function on a subset of belief points representative of the belief space. However, differently from PERSEUS (which is unconstrained), we incorporate the average power constraint via a Lagrangian formulation, and incorporate a dual optimization step to solve the constrained problem. We demonstrate its convergence numerically.
- 4) Inspired by the PERSEUS-based policy, we propose two heuristics with lower computational cost and near-optimal performance, namely belief-based (B-HEU) and finite-

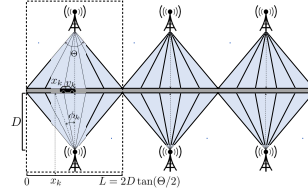


Fig. 1: A cell deployment with BSs on both side of road.

state-machine-based (FSM-HEU) heuristic policies, and analyze the performance of FSM-HEU in closed form.

- 5) We present numerical results for both the idealized *sectorized antenna model* with abstracted mobility model, and a more realistic scenario with analog beamforming and Gauss-Markov mobility. The proposed PERSEUS-based, B-HEU and FSM-HEU are shown to outperform a baseline scheme that performs periodic beam-alignment by a factor 2 in spectral efficiency; additionally, B-HEU and FSM-HEU are shown to achieve near optimal performance (up to 10% degradation with respect to PERSEUS-based), at a fraction of the computational complexity of PERSEUS. Finally, our results depict a good match between the numerical results based on the analysis and the ones based on analog beamforming with Gauss-Markov mobility, thus validating the accuracy of the analysis presented in the paper.

The rest of the paper is organized as follows. In Section II, we introduce the system model, followed by the POMDP formulation in Section III and its optimization in Section IV. In Section V, we present two heuristic policies and analysis of FSM-HEU. We present numerical results in Section VI, followed by concluding remarks in Section VII.

II. SYSTEM MODEL

We consider the scenario of Fig. 1, where multiple base stations (BSs) serve a mobile user (MU) moving along a road. At any time, the MU is associated with one BS – the *serving BS*, which performs data transmission (DT) using beamforming to create a directional link, along with beam training (BT) to maintain alignment. The communication links are subject to time-varying blockages, which cause the signal quality to drop abruptly and DT to fail. As soon as the serving BS detects blockage, it may decide to perform handover (HO) to the BS on the other side of the road, which then continues the process of BT/DT/HO, until either another blockage event is detected, or the MU exits the coverage area of the two BSs.

In this work, we focus on a specific segment of the road link covered by a pair of BSs, as depicted in the framed area of Fig. 1. Within this segment, the BT/DT/HO process continues until the MU exits the coverage area of the two BSs. In this context, we investigate the design of the BT/DT/HO strategy during a transmission episode, defined as the time interval between the two instants when the MU enters and exits the coverage area of the two BSs. The goal is to maximize the average throughput delivered to the MU subject to an average power constraint. Note that, when the episode terminates, the MU enters the coverage area of another pair of BSs, and the same analysis may be applied to each segment traversed.

Both BSs are at a distance D from the road segment, symmetrically with respect to the road, and use a discrete set of narrow beams to communicate with the MU. To this end, the road segment, of length $L \triangleq 2D \tan(\Theta/2)$ and

angular range Θ , is partitioned into N_S sectors of equal length¹ $\Delta_s = L/N_S$, indexed by $s \in \mathcal{S} \equiv \{1, \dots, N_S\}$. Each sector is then associated with one transmission beamformer $\mathbf{c}^{(s)}$, with angular support

$$\Phi_s = \left[\arctan \frac{(s-1)\Delta_s - L/2}{D}, \arctan \frac{s\Delta_s - L/2}{D} \right], \quad \forall s \in \mathcal{S},$$

and beamwidth $\theta_s = |\Phi_s|$. Note that $\cup_{s \in \mathcal{S}} \Phi_s = [-\Theta/2, \Theta/2]$ and $\sum_{s \in \mathcal{S}} \theta_s = \Theta$, so that the ensemble of all beams spans the entire angular region covered by the two BSs.

Time is discretized into time-slots of duration Δ_t , corresponding to the transmission of a beacon signal during BT or of a data fragment during DT. Next, we describe the MU mobility, signal and channel models used throughout the paper.

A. MU Mobility Model

Let $x_k \in [0, L]$ be the position of the MU at time-slot k and

$$S_k = \zeta(x_k) \triangleq s \Leftrightarrow x_k \in [(s-1)\Delta_s, s\Delta_s] \quad (1)$$

be the associated sector index, where $\zeta(\cdot)$ maps the MU position $x_k \in [0, L]$ to sector index $S_k \in \mathcal{S}$. x_k evolves over time according to a random process. Synthetic mobility models proposed in the literature [18], [19] may not adequately represent the specific context operated by the two BSs, thus necessitating the use of a *data-driven model* to characterize the system performance. Since the goal of the two BSs is to perform data communication using one out of S directional beams, it is sufficient to determine the dynamics of $\{S_k, k \geq 0\}$, via the one-step transition probability $\mathbf{P}_{ss'} = \mathbb{P}[S_{k+1} = s' | S_k = s]$, $\forall s, s' \in \mathcal{S}$. To do so: first, N trajectories $\{x_k^{(i)}, 0 \leq k \leq T_i\}$, $i = 1, \dots, N$ are generated according to a given mobility model, or observed in real-time; then, each trajectory is mapped to the sector sequence $\{S_k^{(i)} = \zeta(x_k^{(i)}), 0 \leq k \leq T_i\}$, $i = 1, \dots, N$; finally, letting $\nu_s^{(N)} = \sum_{i=1}^N \sum_{k=0}^{T_i-1} \chi(S_k^{(i)} = s)$ (number of visits to s), $\mathbf{P}_{ss'}$ is estimated as the relative frequency of the $s \rightarrow s'$ transition,

$$\hat{\mathbf{P}}_{ss'}^{(N)} = \frac{1}{\nu_s^{(N)}} \sum_{i=1}^N \sum_{k=0}^{T_i-1} \chi(S_k^{(i)} = s, S_{k+1}^{(i)} = s'), \quad \forall s, s' \in \mathcal{S}, \quad (2)$$

where $\chi(\cdot)$ is the indicator function. $S_k^{(i)}$ may also be estimated from the outcome of the BT scheme (see Sec. II-D), so that the estimate of \mathbf{P} may be improved across several interactions with MUs. Given $\nu_s^{(N)}$, $\hat{\mathbf{P}}^{(N)}$, upon observing a new trajectory $\{S_k^{(N+1)}, 0 \leq k \leq T_{N+1}\}$, $\nu_s^{(N+1)}$ and $\hat{\mathbf{P}}^{(N+1)}$ can be estimated recursively as

$$\nu_s^{(N+1)} = \nu_s^{(N)} + \sum_{k=0}^{T_{N+1}-1} \chi(S_k^{(N+1)} = s), \quad \forall s,$$

$$\hat{\mathbf{P}}_{ss'}^{(N+1)} = \hat{\mathbf{P}}_{ss'}^{(N)} + \frac{1}{\nu_s^{(N+1)}} \sum_{k=0}^{T_{N+1}-1} \chi(S_k^{(N+1)} = s) \left[\chi(S_{k+1}^{(N+1)} = s') - \hat{\mathbf{P}}_{ss'}^{(N)} \right], \quad \forall s, s'.$$

In the following analysis, we assume that \mathbf{P} is known, and we define the absorbing state \bar{s} with $\mathbf{P}_{\bar{s}\bar{s}} = 1$, to model the end of the transmission episode. In Sec. VI, we will present

numerical simulations based on the Gauss-Markov mobility model [19], with \mathbf{P} estimated as in (2).

B. Signal and Channel Models

Within the k th time-slot, L symbols are transmitted by the serving BS, denoted with the index $I_k \in \{1, 2\}$. Let $\mathbf{x}_k \in \mathbb{C}^L$ be the transmitted signal with $\mathbb{E}[\|\mathbf{x}_k\|_2^2] = L$. Assuming isotropic MU, its received signal is expressed as

$$\mathbf{y}_k = \sqrt{P_k} \mathbf{h}_k \mathbf{c}_k \mathbf{x}_k + \mathbf{w}_k, \quad (3)$$

where P_k is the average transmit power of the serving BS; $\mathbf{h}_k \in \mathbb{C}^{1 \times M_{\text{tx}}}$ is the channel vector; M_{tx} is the number of antenna elements at each BS; $\mathbf{c}_k \in \mathbb{C}^{M_{\text{tx}} \times 1}$ with $\|\mathbf{c}_k\|_2^2 = 1$ is the analog beamforming vector; $\mathbf{w}_k \sim \mathcal{CN}(0, \sigma_w^2 \mathbf{I})$ with $\sigma_w^2 = (1 + F)N_0W_{\text{tot}}$ is additive white Gaussian noise (AWGN), N_0 is the noise power spectral density, W_{tot} is the signal bandwidth and F is the noise figure of the receiver.

In this paper, we model \mathbf{h}_k as a single line of sight (LOS) path with binary blockage [20] and diffuse multipath components [21],

$$\mathbf{h}_k = \underbrace{\sqrt{M_{\text{tx}}} B_k^{(I_k)} h_k \mathbf{d}_{\text{tx}}(\psi_k)^H}_{\mathbf{h}_k^{\text{LOS}}} + \underbrace{\sum_{l=1}^{N_{\text{DIF}}} \sqrt{M_{\text{tx}}} h_{k,l}^{\text{DIF}} \mathbf{d}_{\text{tx}}(\psi_{k,l}^{\text{DIF}})^H}_{\mathbf{h}_k^{\text{DIF}}}, \quad (4)$$

where $B_k^{(i)} \in \{0, 1\}$ denotes the binary blockage variable of BS i , equal to 1 if the LOS path is unobstructed, equal to zero otherwise; $\mathbf{d}_{\text{tx}}(\psi_k) \in \mathbb{C}^{M_{\text{tx}}}$ is the BS array response vector, and $\psi_k \triangleq \sin(\phi_k) = (x_k - L/2)/d(\phi_k)$ is the spatial angle corresponding to the angle of departure (AoD), computed with respect to the perpendicular to the array) $\phi_k \in [-\Theta/2, \Theta/2]$; $h_k \sim \mathcal{CN}(0, \sigma_h^2)$ is the complex channel gain of the LOS component, i.i.d. over slots, with $\sigma_h^2 = 1/\ell(\phi_k)$; $\ell(\phi_k) = (\frac{4\pi d(\phi_k)}{\lambda_c})^2$ denotes the path loss as function BS-MU distance $d(\phi_k) = D\sqrt{1 + \tan^2(\phi_k)}$ (see Fig. 1); $\lambda_c = c/f_c$ is the wavelength. Finally, $\mathbf{h}_k^{\text{DIF}}$ denotes the channel corresponding to diffuse multipath components with coefficients $h_{k,l}^{\text{DIF}}$ and AoD $\psi_{k,l}^{\text{DIF}}$; we model $\mathbf{h}_k^{\text{DIF}}$ as zero-mean complex Gaussian, with i.i.d. entries (over time and over antennas), each with variance σ_{DIF}^2 , $\mathbf{h}_k^{\text{DIF}} \sim \mathcal{CN}(\mathbf{0}, \sigma_{\text{DIF}}^2 \mathbf{I})$. These components have been shown to be much weaker than the LOS path (up to 100× weaker at a BS-MU distance of only 10 meters [20]), so that $\sigma_{\text{DIF}}^2 \ll \sigma_h^2$. For uniform linear arrays (ULAs) with antenna spacing d_c , \mathbf{d}_{tx} is expressed as

$$\mathbf{d}_{\text{tx}}(\psi_k) = \frac{1}{\sqrt{M_{\text{tx}}}} \left[1, e^{j\frac{2\pi d_c}{\lambda_c} \psi_k}, \dots, e^{j\frac{2\pi d_c}{\lambda_c} (M_{\text{tx}}-1)\psi_k} \right]^T. \quad (5)$$

Then, letting $G_{\text{tx}}(\mathbf{c}, \phi) = M_{\text{tx}} |\mathbf{d}_{\text{tx}}(\sin \phi)^H \mathbf{c}|^2$ be the beamforming gain of the serving BS and $\Theta_{\text{tx}} = \angle \mathbf{d}_{\text{tx}}(\psi)^H \mathbf{c}$ be its phase, the signal received at the MU can be expressed as

$$\mathbf{y}_k = \sqrt{P_k} \left[B_k^{(I_k)} h_k \sqrt{G_{\text{tx}}(\mathbf{c}_k, \phi_k)} e^{j\Theta_{\text{tx}}} + \Omega_k \right] \mathbf{x}_k + \mathbf{w}_k, \quad (6)$$

where $\Omega_k \triangleq \mathbf{h}_k^{\text{DIF}} \mathbf{c}_k \sim \mathcal{CN}(0, \sigma_{\text{DIF}}^2)$ is the contribution due to the diffuse multipath channel components. The SNR averaged over the fading coefficients is given as

$$\text{SNR}_k = B_k^{(I_k)} \frac{P_k G(\mathbf{c}_k, \phi_k)}{\sigma_w^2 \ell(\phi_k)} + \frac{P_k \sigma_{\text{DIF}}^2}{\sigma_w^2}. \quad (7)$$

¹The equal length assumption is made for the sake of notational convenience. However, the analysis is valid for non-uniform length sectors.

The blockage state $B_k^{(i)}$ evolves over time as a binary Markov chain with transition probabilities

$$\mathbb{P}_{b \rightarrow b'}^{(i)} = \mathbb{P}(B_{k+1}^{(i)} = b' | B_k^{(i)} = b). \quad (8)$$

Since the two BSs are on opposite sides of the road, they experience different types of obstructions to the MU. We thus model the processes $\{B_k^{(i)}, k \geq 0\}, i \in \{1, 2\}$ as independent of each other, with Markov dynamics (8).

C. Sectored antenna model

In this paper, we use the *sectored antenna model* to approximate the BS beamforming gain $G_{\text{tx}}(\mathbf{c}^{(s)}, \sin(\phi))$, as also used in [8], [17]. As we will show in Section VI, when coupled with appropriate design of the beamforming vector $\mathbf{c}^{(s)}$ [22], the sectored model provides an accurate and analytically tractable approximation of the actual beamforming gain.

Consider the s -th beam spanning the s -th sector, with angular support Φ_s and beamforming vector $\mathbf{c}^{(s)}$. Under the sectored model, the beamforming gain is such that $G_{\text{tx}}(\mathbf{c}^{(s)}, \phi) \approx g_s \ll 1$ in the sidelobe ($\forall \phi \notin \Phi_s$) and $G_{\text{tx}}(\mathbf{c}^{(s)}, \phi) \gg 1$ in the main-lobe, with gain-to-pathloss ratio $G_{\text{tx}}(\mathbf{c}^{(s)}, \phi)/\ell(\phi) \approx \Upsilon_s, \forall \phi \in \Phi_s$. Based on this model, we now derive expressions for the transmission power to achieve a target SNR at the receiver. We denote the case in which the MU is in the mainlobe with no blockage ($\phi \in \Phi_s$ and $B_k^{(I_k)} = 1$) as "active beam"; we denote the complementary case of blockage or MU in the sidelobe ($\phi \notin \Phi_s$ or $B_k^{(I_k)} = 0$) as "no active beam." In the case of active beam, from (7) we have

$$\text{SNR} = \frac{P_s \Upsilon_s}{\sigma_w^2} + \frac{P_s \sigma_{\text{DIF}}^2}{\sigma_w^2} \simeq \frac{P_s \Upsilon_s}{\sigma_w^2} \Leftrightarrow P_s = \frac{\sigma_w^2}{\Upsilon_s} \text{SNR}, \quad (9)$$

where we note that $\sigma_{\text{DIF}}^2 \ll \sigma_h^2 G_{\text{tx}}(\mathbf{c}^{(s)}, \phi) \approx \Upsilon_s, \forall \phi \in \Phi_s$, i.e., the signal strength of the LOS component is much larger than diffuse multipath components within the mainlobe. Otherwise, in case of no active beam we find that

$$\begin{aligned} \text{SNR}_{k=B_k^{(I_k)}} &= \frac{P_s \Upsilon_s}{\sigma_w^2} \frac{G(\mathbf{c}^{(s)}, \phi)}{\ell(\phi) \Upsilon_s} + \frac{P_s \sigma_{\text{DIF}}^2}{\sigma_w^2} \\ &= \left[B_k^{(I_k)} \frac{G(\mathbf{c}^{(s)}, \phi)}{\ell(\phi) \Upsilon_s} + \frac{\sigma_{\text{DIF}}^2}{\Upsilon_s} \right] \text{SNR}, \quad \forall \phi \notin \Phi_s. \end{aligned} \quad (10)$$

Herein, we use a worst-case approximation of the SNR for detection performance in the case of no active beam,

$$\text{SNR}_k \leq \max_{s \in \mathcal{S}} \max_{\phi \notin \Phi_s} \left[\frac{G(\mathbf{c}^{(s)}, \phi)}{\ell(\phi) \Upsilon_s} + \frac{\sigma_{\text{DIF}}^2}{\Upsilon_s} \right] \text{SNR} \triangleq \rho \text{SNR}, \quad (11)$$

maximized over $B_k^{(I_k)} \in \{0, 1\}$, sector s and sidelobe angle ϕ . In other words, to achieve a target SNR within the mainlobe of sector s , the BS should transmit with power given by (9); however, if the signal is blocked or the MU is on the sidelobe (or both), the associated worst-case SNR is ρSNR . Note that, in this case, data transmission is in outage since $\rho \ll 1$ (numerically, we found $\rho = -22\text{dB}$). In addition, the larger ρ , the more difficult it is for the BS to detect whether the signal is blocked or not, or whether the MU is in the mainlobe or sidelobe; for this reason, ρ is defined by maximizing the SNR over all possible sidelobe and blockage states as in (11).

D. Beam Training (BT) and Data Transmission (DT)

We now introduce the BT and DT operations performed by the serving BS. We let $(S_k, I_k, B_k^{(1)}, B_k^{(2)})$ be the state of the system in time-slot k , where $S_k \in \mathcal{S}$ denotes the index of the sector occupied by the MU, I_k is the index of the serving BS, and $B_k^{(i)} \in \{0, 1\}$ is the blockage state of the i th BS.

BT phase: At the start of a BT phase, the BS selects a set of sectors $\hat{\mathcal{S}}_{\text{BT}}$ over which it will send the beacons \mathbf{x}_k for BT, and a target SNR SNR_{BT} . The beacon transmission is done in sequence, using one slot for each sector in the set $\hat{\mathcal{S}}_{\text{BT}}$. Therefore, the duration of the BT phase is $T_{\text{BT}} \triangleq |\hat{\mathcal{S}}_{\text{BT}}| + 1$, including the last slot for feedback signaling from the MU to the BS. Let $i \in \{0, \dots, T_{\text{BT}} - 2\}$ be the i th timeslot of the BT phase, and $\hat{s}_i \in \hat{\mathcal{S}}_{\text{BT}}$ be the sector scanned by the BS. The MU processes the received signal \mathbf{y}_{k+i} with a matched filter,

$$z_{\hat{s}_i} \triangleq \frac{|\mathbf{x}_{k+i}^H \mathbf{y}_{k+i}|^2}{(1+F)N_0 W_{\text{tot}} \|\mathbf{x}_{k+i}\|_2^2}. \quad (12)$$

Upon collecting the sequence $\{z_{\hat{s}_i}, \forall \hat{s}_i \in \hat{\mathcal{S}}_{\text{BT}}\}$, the MU generates the feedback signal

$$Y = \begin{cases} \hat{s}^* \triangleq \arg \max_{\hat{s} \in \hat{\mathcal{S}}_{\text{BT}}} z_{\hat{s}}, & \max_{\hat{s} \in \hat{\mathcal{S}}_{\text{BT}}} z_{\hat{s}} > \eta_{\text{BT}}, \\ \emptyset, & \max_{\hat{s} \in \hat{\mathcal{S}}_{\text{BT}}} z_{\hat{s}} \leq \eta_{\text{BT}}. \end{cases} \quad (13)$$

In other words, if all the matched filter outputs are weaker than η_{BT} , $Y = \emptyset$ indicates that no beam is deemed sufficient for data transmission, either due to blockage ($B_k^{(I)} = 0$), or the MU being located outside of the BT beams ($S_k \notin \hat{\mathcal{S}}_{\text{BT}}$). Otherwise, $Y = \hat{s}^*$ indicates the ID of the strongest beam detected.

We now perform a probabilistic analysis of the feedback. To this end, we assume that the state variables do not change during the transmission of the beacon sequences, i.e., $(S_{k+i}, I_{k+i}, B_{k+i}^{(1)}, B_{k+i}^{(2)}) = (s, I, b_1, b_2), \forall i \in \{0, \dots, T_{\text{BT}} - 2\}$. This is a reasonable assumption, since the duration of the BT phase ($\times 0.1\text{ms}$) is typically much shorter than the time required by the MU to change sector ($\times 100\text{ms}$) or the timescales of blockage ($\times 100\text{ms}$). With this assumption, given the system state (s, I, b_1, b_2) during BT, the signal sequence $\{z_{\hat{s}}, \forall \hat{s} \in \hat{\mathcal{S}}_{\text{BT}}\}$ is independent across \hat{s} , due to the i.i.d. nature of h_{k+i} and \mathbf{w}_{k+i} . In addition, in case of active beam ($s = \hat{s}$ and $b_I = 1$), by using (6) and (9), $z_{\hat{s}}$ has exponential distribution with mean $1 + \text{SNR}_{\text{BT}} L$, $z_{\hat{s}} \sim \mathcal{E}(1 + \text{SNR}_{\text{BT}} L)$; otherwise (no active beam, $s \neq \hat{s}$ or $b_I = 0$) $z_{\hat{s}} \sim \mathcal{E}(1 + \rho \text{SNR}_{\text{BT}} L)$. Now, let us consider separately the two events $\{s \notin \hat{\mathcal{S}}_{\text{BT}}\} \cup \{b_I = 0\}$ and $\{s \in \hat{\mathcal{S}}_{\text{BT}}\} \cap \{b_I = 1\}$, denoted respectively as "no active beam in $\hat{\mathcal{S}}_{\text{BT}}$ " or "active beam in $s \in \hat{\mathcal{S}}_{\text{BT}}$ ". It follows that

$$\begin{aligned} \Sigma_\rho &\triangleq \mathbb{P}(z_{\hat{s}} \leq \eta_{\text{BT}} | \text{active beam in } s) = 1 - e^{-\frac{\eta_{\text{BT}}}{1 + \rho \text{SNR}_{\text{BT}} L}}, \quad \forall \hat{s} \neq s, \\ \Sigma_1 &\triangleq \mathbb{P}(z_s \leq \eta_{\text{BT}} | \text{active beam in } s) = 1 - e^{-\frac{\eta_{\text{BT}}}{1 + \text{SNR}_{\text{BT}} L}}. \end{aligned}$$

If there is no active beam in $\hat{\mathcal{S}}_{\text{BT}}$, then the probability of generating the feedback signal $Y = \emptyset$ (i.e., of correctly detecting no active beams within the sectors scanned in the BT phase) is

$$\begin{aligned} \mathbb{P}(Y = \emptyset | \text{no active beam in } \hat{\mathcal{S}}_{\text{BT}}) &= \prod_{\hat{s} \in \hat{\mathcal{S}}_{\text{BT}}} \mathbb{P}(z_{\hat{s}} \leq \eta_{\text{BT}} | \text{no active beam in } \hat{s}) = \Sigma_\rho^{|\hat{\mathcal{S}}_{\text{BT}}|}, \end{aligned} \quad (14)$$

since $Y = \emptyset$ is equivalent to $z_{\hat{s}} \leq \eta_{BT}, \forall \hat{s} \in \hat{\mathcal{S}}_{BT}$, and $z_{\hat{s}}$ are independent across \hat{s} , conditional on the system state. Similarly, if there is an active beam in $s \in \hat{\mathcal{S}}_{BT}$, the probability of incorrectly detecting no active beam is

$$\begin{aligned} \mathbb{P}(Y = \emptyset | \text{active beam in } s \in \hat{\mathcal{S}}_{BT}) & \quad (15) \\ &= \prod_{\hat{s} \in \hat{\mathcal{S}}_{BT}} \mathbb{P}(z_{\hat{s}} \leq \eta_{BT} | \text{active beam in } s \in \hat{\mathcal{S}}_{BT}) = \Sigma_1 \Sigma_\rho^{|\hat{\mathcal{S}}_{BT}|-1}, \end{aligned}$$

since $z_s \sim \mathcal{E}(1 + \text{SNR}_{BT}L)$ for sector s occupied by the MU.

If there is no active beam in $\hat{\mathcal{S}}_{BT}$, the probability of generating the feedback signal \hat{s}^* (i.e., of detecting incorrectly that a strong beam is available) is

$$\begin{aligned} \mathbb{P}(Y = \hat{s}^* | \text{no active beam in } \hat{\mathcal{S}}_{BT}) & \quad (16) \\ &= \frac{1}{|\hat{\mathcal{S}}_{BT}|} \left[1 - \mathbb{P}(Y = \emptyset | \text{no active beam in } \hat{\mathcal{S}}_{BT}) \right] = \frac{1 - \Sigma_\rho^{|\hat{\mathcal{S}}_{BT}|}}{|\hat{\mathcal{S}}_{BT}|}; \end{aligned}$$

in fact, $z_{\hat{s}}$ are i.i.d. across beams, conditional on no active beam, so that incorrect detections are uniform across the feedback outcomes $\hat{s}^* \in \hat{\mathcal{S}}_{BT}$.

Instead, when there is an active beam in $\hat{\mathcal{S}}_{BT}$, we need to further distinguish between the two cases $s = \hat{s}^*$ (the strongest beam is detected correctly) and $s \neq \hat{s}^*$ (incorrect detection). The probability of correctly detecting the strongest beam is

$$\begin{aligned} \mathbb{P}(Y = s | \text{active beam in } s \in \hat{\mathcal{S}}_{BT}) & \quad (17) \\ &= \mathbb{P}(z_s > \eta_{BT}, z_s > z_{\hat{s}}, \forall \hat{s} \in \hat{\mathcal{S}}_{BT} \setminus \{s\} | \text{active beam in } s \in \hat{\mathcal{S}}_{BT}) \\ &= \int_{\eta_{BT}}^{\infty} \left[\frac{1}{1 + \text{SNR}_{BT}L} \exp \left\{ -\frac{\tau}{1 + \text{SNR}_{BT}L} \right\} \right. \\ & \quad \times \left. \left(1 - \exp \left\{ -\frac{\tau}{1 + \rho \text{SNR}_{BT}L} \right\} \right)^{|\hat{\mathcal{S}}_{BT}|-1} \right] d\tau \\ &= \sum_{n=0}^{|\hat{\mathcal{S}}_{BT}|-1} \binom{|\hat{\mathcal{S}}_{BT}|-1}{n} \frac{(-1)^n}{1 + \frac{1 + \text{SNR}_{BT}L}{1 + \rho \text{SNR}_{BT}L} n} (1 - \Sigma_1)(1 - \Sigma_\rho)^n, \end{aligned}$$

where in the first step we used the definition of $Y = s$, i.e., z_s must be greater than the threshold η_{BT} , and all other $z_{\hat{s}}$ must be smaller than z_s ; in the last step, we used Newton's binomial theorem to solve the integral. Finally, the probability of incorrectly detecting the strongest beam $\hat{s}^* \neq s$ is

$$\begin{aligned} \mathbb{P}(Y = \hat{s}^* | \text{active beam in } s \in \hat{\mathcal{S}}_{BT}) & \quad (18) \\ &= \frac{1}{|\hat{\mathcal{S}}_{BT}|-1} \left[1 - \sum_{y \in \{s, \emptyset\}} \mathbb{P}(Y = y | \text{active beam in } s \in \hat{\mathcal{S}}_{BT}) \right] \end{aligned}$$

since, similarly to (16), erroneous detections are uniform across the remaining $|\hat{\mathcal{S}}_{BT}|-1$ sectors.

Since $Y = \emptyset$ represents no active beam detected, we choose η_{BT} so that the misdetection and false alarm probabilities are both equal to δ_{BT} , yielding from (15)-(16) (over all $\hat{s} \in \hat{\mathcal{S}}_{BT}$),

$$\delta_{BT} = 1 - \Sigma_\rho^{|\hat{\mathcal{S}}_{BT}|} = \Sigma_1 \Sigma_\rho^{|\hat{\mathcal{S}}_{BT}|-1}. \quad (19)$$

The value of η_{BT} and the corresponding δ_{BT} for a given SNR_{BT} and $|\hat{\mathcal{S}}_{BT}|$ can be found numerically using the bisection method, since the left- and right- hand sides of (19) are decreasing and increasing functions of η_{BT} , respectively.

DT phase: At the start of the DT phase, the BS chooses a sector $\hat{s} \in \mathcal{S}$ used for data transmission, along with the duration

T_{DT} of the DT frame, the target average SNR at the receiver SNR_{DT} , and a target transmission rate \bar{R}_{DT} ; the last slot is used for the feedback signal from the MU to the BS, as described below. We assume that a fixed fraction $\kappa \in (0, 1)$ out of L symbols in each slot is used for channel estimation. Then, if an active beam is present in \hat{s} , and assuming that channel estimation errors are negligible compared to the noise level (achieved with a sufficiently long pilot sequence κL), from the signal model (6), we find that outage occurs if

$$W_{\text{tot}} \log_2(1 + |h_k|^2 \ell(d_k) \text{SNR}_{DT}) < \bar{R}_{DT}, \quad (20)$$

(note that $\mathbb{E}[|h_k|^2 \ell(d_k)] = 1$) yielding the outage probability

$$\begin{aligned} \mathbb{P}_{\text{OUT}}(\bar{R}_{DT}, \text{SNR}_{DT}) &= \mathbb{P}\left(|h_k|^2 \ell(d_k) < \frac{2^{\bar{R}_{DT}/W_{\text{tot}}} - 1}{\text{SNR}_{DT}}\right) \\ &= 1 - \exp\left\{-\frac{2^{\bar{R}_{DT}/W_{\text{tot}}} - 1}{\text{SNR}_{DT}}\right\}. \quad (21) \end{aligned}$$

In this paper, we design \bar{R}_{DT} based on the notion of ϵ -outage capacity, i.e., \bar{R}_{DT} is the largest rate such that $\mathbb{P}_{\text{OUT}}(\bar{R}_{DT}, \text{SNR}_{DT}) \leq \epsilon$, for a target outage probability $\epsilon < 1$. Forcing (21) equal to ϵ , this can be expressed as

$$\bar{R}_{DT} = C_\epsilon(\text{SNR}_{DT}) = W_{\text{tot}} \log_2(1 - \text{SNR}_{DT} \ln(1 - \epsilon)). \quad (22)$$

In other words, the transmission is successful with probability $1 - \epsilon$, and the average rate (throughput) is

$$\mathcal{T}(\epsilon, \text{SNR}_{DT}) \triangleq (1 - \kappa)(1 - \epsilon)C_\epsilon(\text{SNR}_{DT}), \quad (23)$$

where $(1 - \kappa)$ accounts for the channel estimation overhead. In the sequel, we select ϵ to maximize the throughput, yielding the optimal $\epsilon^*(\text{SNR}_{DT})$ at a given SNR SNR_{DT} as the unique fixed point of $d\mathcal{T}(\epsilon, \text{SNR}_{DT})/d\epsilon = 0$, or equivalently,

$$\ln(1 - \text{SNR}_{DT} \ln(1 - \epsilon)) \left(1 - \text{SNR}_{DT} \ln(1 - \epsilon)\right) = \text{SNR}_{DT}.$$

We denote the resulting throughput maximized over ϵ as $\mathcal{T}^*(\text{SNR}_{DT}) \triangleq \mathcal{T}(\epsilon^*(\text{SNR}_{DT}), \text{SNR}_{DT})$.

In this paper, we envision a mechanism in which the pilot signal transmitted in the second last slot of the DT phase is used to generate the binary feedback signal

$$Y = \begin{cases} \hat{s}, & z_{\hat{s}} > \eta_{DT} \\ \emptyset, & z_{\hat{s}} \leq \eta_{DT}, \end{cases} \quad (24)$$

transmitted by the MU to the BS in the last slot of the DT phase. As in (12) for the BT feedback, $Y = \hat{s}$ denotes active beam detected, whereas $Y = \emptyset$ denotes no active beam, due to either loss of alignment or blockage. Similarly to (12),

$$z_{\hat{s}} \triangleq \frac{|\mathbf{x}_{k+T_{DT}-2}^{(p)H} \mathbf{y}_{k+T_{DT}-2}^{(p)}|^2}{(1 + F)N_0 W_{\text{tot}} \|\mathbf{x}_{k+T_{DT}-2}^{(p)}\|_2^2}$$

is based on the pilot signal $\mathbf{x}_{k+T_{DT}-2}^{(p)}$ (of duration κL) and on the corresponding signal $\mathbf{y}_{k+T_{DT}-2}^{(p)}$ received on the second last slot of the DT phase. The distribution of the feedback conditional on $(S_t, I_t, B_t^{(1)}, B_t^{(2)}) = (s, I, b_1, b_2)$ at time $t = k + T_{DT} - 2$ (second last slot) can be computed as a special case of (15) and (16) with $|\hat{\mathcal{S}}_{BT}| = 1$ (since in the DT phase only one sector \hat{s} is used for data transmission) and κL in place of L (since only a fraction κ out of L symbols is used for the pilot signal), yielding the probability of incorrectly detecting

an active beam as

$$\mathbb{P}(Y=\hat{s}|\text{no active beam in } \hat{s})=\exp\left\{-\frac{\eta_{DT}}{1+\rho\kappa\text{SNR}_{DT}L}\right\}, \quad (25)$$

and the probability of incorrectly detecting no active beam as

$$\mathbb{P}(Y=\emptyset|\text{active beam in } \hat{s})=1-\exp\left\{-\frac{\eta_{DT}}{1+\kappa\text{SNR}_{DT}L}\right\}. \quad (26)$$

As in the BT phase, we choose η_{DT} so that the probabilities of misdetection and false alarm are both equal to δ_{DT} , yielding

$$\delta_{DT}=\exp\left\{\frac{-\eta_{DT}}{1+\rho\kappa\text{SNR}_{DT}L}\right\}=1-\exp\left\{\frac{-\eta_{DT}}{1+\kappa\text{SNR}_{DT}L}\right\}. \quad (27)$$

III. POMDP FORMULATION

We now formulate the problem of optimizing the BT, DT and HO strategy as a constrained POMDP. In the following, we define the elements of this POMDP.

States: the state is denoted as $u_k \triangleq (S_k, I_k, B_k^{(1)}, B_k^{(2)}) \in \mathcal{U}$ taking values from the set $\mathcal{U}=(\mathcal{S} \times \{1, 2\} \times \{0, 1\}^2)$, where $S_k \in \mathcal{S}$ is the position of the MU within the road segment, $I_k \in \{1, 2\}$ is the index of the serving BS, and $B_k^{(i)} \in \{0, 1\}$ is the blockage state of BS $i \in \{1, 2\}$. With the absorbing state \bar{s} to denote the episode termination, the overall state space is then $\bar{\mathcal{U}}=\mathcal{U} \cup \{\bar{s}\}$.

Actions: the serving BS can perform three actions: beam training (BT), data transmission (DT), or handover (HO). However, differently from standard POMDPs in which each action takes one slot, in this paper we generalize the model to actions taking multiple slots, as explained next.

If action HO is chosen, the data plane is transferred to the other BS, which becomes the serving one for the successive time-slots, until HO is chosen again. This action requires T_{HO} time-slots to be completed, modeling the delay to coordinate the transfer of the data traffic between the two BSs.

If actions BT is chosen, the serving BS chooses the set $\hat{\mathcal{S}}$ of sectors to scan and the target SNR SNR_{BT} . The transmission power is then found via (9), and the feedback error probability δ_{BT} is found by solving (19). The duration of the BT action is $T_{BT} = |\hat{\mathcal{S}}|+1: |\hat{\mathcal{S}}|$ slots for scanning the set of sectors $\hat{\mathcal{S}}$, and one slot for the feedback from the MU to the serving BS.

If action DT is chosen, then the serving BS selects the sector \hat{s} covered during data communication, along with the duration $T_{DT} \geq 2$ of the data communication session, and the target SNR SNR_{DT} . The transmission power is then determined via (9), and the transmission rate is given by (22) to achieve ϵ -outage capacity, so that the resulting expected throughput (in case of LOS and correct alignment) is $\mathcal{T}^*(\text{SNR}_{DT})$. The duration of the data communication session T_{DT} includes the second last slot to generate the feedback signal, which is transmitted from the MU to the BS in the last slot. The feedback error probability δ_{DT} is the unique fixed point of (27).

We represent compactly these actions as $(c, \Pi_c) \in \mathcal{A}$, with action space \mathcal{A} , where $c \in \{\text{BT}, \text{DT}, \text{HO}\}$ refers to the action class and $\Pi_c = (\hat{\mathcal{S}}, \text{SNR}, T)$ specifies the corresponding parameters: $\hat{\mathcal{S}} \subseteq \mathcal{S}$ is a sub-set of sectors, used during the action, SNR is the target SNR, so that the transmission power of the corresponding action is given by (9), and T is the action duration. Specifically, $T = |\hat{\mathcal{S}}|+1$ for a BT action, $\hat{\mathcal{S}} = \{\hat{s}\}$ for a DT action, and $\Pi_c = (\emptyset, 0, T_{HO})$ for an HO action.

Observations: upon selecting action $A_k \in \mathcal{A}$ of duration T in slot k and executing it in state $u_k \in \mathcal{U}$, the BS observes Y_k from the set $\mathcal{Y}=\mathcal{S} \cup \{\emptyset\} \cup \{\bar{s}\}$. $Y_k=\bar{s}$ denotes that the MU exited the coverage area of the two BSs, hence the episode terminates; otherwise, Y_k denotes the feedback signal after the action is completed, as described earlier for the BT and DT actions in (13) and (24) (we set $Y_k=\emptyset$ under the HO action).

Transition and Observation probabilities: Let $\mathbb{P}(U_{k+T} = u', Y_k = y | U_k = u, A_k = a)$ be the probability of moving from state $u \in \mathcal{U}$ to state $u' \in \bar{\mathcal{U}}$ and observing $y \in \mathcal{Y}$ under action $a \in \mathcal{A}$ of duration T . To derive it, let $u = (s, I, b_1, b_2)$ be the current state, $a = (c, \Pi_c)$ be the selected action and $y \in \mathcal{Y}$ be the observation. It is useful to define the T -steps transition probability of the MU from s to s' as

$$\mathbf{S}_{ss'}(T) \triangleq \mathbb{P}(S_{k+T}=s' | S_k=s) = [\mathbf{P}^T]_{ss'}, \quad \forall s' \in \mathcal{S} \cup \{\bar{s}\},$$

and the T -steps transition probability of the blockage state of BS i from b_i to b'_i as

$$\mathbf{B}_{bb'}^{(i)}(T) \triangleq \mathbb{P}(B_{k+T}^{(i)} = b' | B_k^{(i)} = b).$$

Letting $\mu_i \triangleq 1 - \mathbb{P}_{1 \rightarrow 0}^{(i)} - \mathbb{P}_{0 \rightarrow 1}^{(i)}$, this is given in closed form as

$$\begin{aligned} \mathbf{B}_{10}^{(i)}(T) &= \pi_0^{(i)} (1 - \mu_i^T), \quad \mathbf{B}_{11}^{(i)}(T) = \pi_1^{(i)} + \pi_0^{(i)} \mu_i^T, \\ \mathbf{B}_{01}^{(i)}(T) &= \pi_1^{(i)} (1 - \mu_i^T), \quad \mathbf{B}_{00}^{(i)}(T) = \pi_0^{(i)} + \pi_1^{(i)} \mu_i^T, \end{aligned} \quad (29)$$

where we have defined the steady state probabilities of $B_k^{(i)}$ being blocked ($\pi_0^{(i)}$) or LOS ($\pi_1^{(i)}$) as

$$\pi_1^{(i)} = \frac{\mathbb{P}_{0 \rightarrow 1}^{(i)}}{\mathbb{P}_{0 \rightarrow 1}^{(i)} + \mathbb{P}_{1 \rightarrow 0}^{(i)}}, \quad \pi_0^{(i)} = \frac{\mathbb{P}_{1 \rightarrow 0}^{(i)}}{\mathbb{P}_{0 \rightarrow 1}^{(i)} + \mathbb{P}_{1 \rightarrow 0}^{(i)}}. \quad (30)$$

If $u' = \bar{s}$ (episode termination), then the observation signal is deterministically $Y_k = \bar{s}$, so that we obtain

$$\mathbb{P}(U_{k+T}=\bar{s}, Y_k=\bar{s} | U_k=u, A_k=a) = \mathbf{S}_{s\bar{s}}(T), \quad (31)$$

i.e., it is equivalent to the probability of exiting the coverage area of the two BSs in T steps.

We now focus on the case $u' \neq \bar{s}$, i.e., the MU is still within the coverage area, and let $u' = (s', I', b'_1, b'_2)$ be the next state. Under the HO action $a = (\text{HO}, \emptyset, 0, T_{HO})$, of duration $T = T_{HO}$, then necessarily $I' \neq I$ as a result of the handover operation, and the observation signal is deterministically $Y_k = \emptyset$, yielding

$$\begin{aligned} &\mathbb{P}(U_{k+T}=(s', I', b'_1, b'_2), Y_k = \emptyset | U_k=(s, I, b_1, b_2), A_k=a) \\ &= \mathbf{S}_{ss'}(T) \mathbf{B}_{b_1 b'_1}^{(1)}(T) \mathbf{B}_{b_2 b'_2}^{(2)}(T), \end{aligned} \quad (32)$$

i.e., the MU moves from s to s' in T steps, and the blockage state of BS i moves from b_i to b'_i in T slots. The expression given above is due to the facts that the mobility of the MU is independent of blockage events, and blockages of the two BSs are independent of each other.

Under the BT action $a = (\text{BT}, \hat{\mathcal{S}}, \text{SNR}, T)$, of duration $T = |\hat{\mathcal{S}}|+1$, then necessarily $I' = I$ (no handover), and the observation signal is $Y_k = y \in \hat{\mathcal{S}} \cup \{\emptyset\}$ (see the signaling mechanism defined in the BT phase in Sec. II). Therefore,

$$\begin{aligned} &\mathbb{P}(U_{k+T}=(s', I, b'_1, b'_2), Y=y | U_k=(s, I, b_1, b_2), A_k=a) \\ &= \mathbb{P}(Y=y | \hat{\mathcal{S}}, S_k=s, B_k^{(I)}=b_I) \mathbf{S}_{ss'}(T) \mathbf{B}_{b_1 b'_1}^{(1)}(T) \mathbf{B}_{b_2 b'_2}^{(2)}(T), \end{aligned} \quad (33)$$

$$\begin{aligned}
& \mathbb{P}\left(U_{k+T} = (s', I, b'_1, b'_2), Y_k = y | U_k = (s, I, b_1, b_2), A_k = a\right) \\
&= \sum_{s'' \in \mathcal{S}, b''_I \in \{0,1\}} \mathbb{P}\left(U_{k+T} = (s', I, b'_1, b'_2), Y = y, S_{k+T-2} = s'', B_{k+T-2}^{(I)} = b''_I | U_k = (s, I, b_1, b_2), A_k = a\right) \\
&= \mathbf{B}_{b_J b'_J}^{(J)}(T) \sum_{s'' \in \mathcal{S}, b''_I \in \{0,1\}} \left[\mathbf{S}_{s s''}(T-2) \mathbf{B}_{b_I b''_I}^{(I)}(T-2) \mathbb{P}\left(Y = y | \hat{s}, S_{k+T-2} = s'', B_{k+T-2}^{(I)} = b''_I\right) \mathbf{S}_{s'' s'}(2) \mathbf{B}_{b'_1 b'_2}^{(I)}(2) \right] \quad (28)
\end{aligned}$$

where $\mathbb{P}(Y=y|\hat{S}, S_k=s, B_k^{(I)}=b_I)$ has been defined in (14)-(18) for the cases of active beam $s \in \hat{\mathcal{S}}$ and no active beam.

Finally, under the DT action $a=(\text{DT}, \{\hat{s}\}, \text{SNR}, T)$, then necessarily $I'=I$ (no handover), and the observation signal is $Y_k=y \in \{\hat{s}, \emptyset\}$ (see the signaling mechanism defined in the DT phase in Sec. II). However, in this case the feedback signal is generated based on the second last slot, i.e., it depends on the state U_{k+T-2} at time $k+T-2$. By computing the marginal with respect to $S_{k+T-2}=s''$ and $B_{k+T-2}^{(I)}=b''_I$, we then obtain (28) given on top of this page. In (28), $\mathbb{P}(Y=y|\hat{s}, S_{k+T-2}=s'', B_{k+T-2}^{(I)}=b''_I)$ was derived in (25), (26) for the cases of active beam in s or no active beam in s , and $J \neq I$ denotes the non-serving BS. To explain (28), note that: the system moves from $(S_k, B_k^{(I)})=(s, b_I)$ to $(S_{k+T-2}, B_{k+T-2}^{(I)})=(s'', b''_I)$ in $T-2$ steps; at this point, the feedback signal is generated with distribution $\mathbb{P}(Y=y|\hat{s}, S_{k+T-2}=s'', B_{k+T-2}^{(I)}=b''_I)$; finally, the system moves from $(S_{k+T-2}, B_{k+T-2}^{(I)})=(s'', b''_I)$ to $(S_{k+T}, B_{k+T}^{(I)})=(s', b'_I)$ in the remaining 2 steps.

Costs and Rewards: for every state action pair (u, a) , we let $r(u, a)$ and $e(u, a)$ be the expected number of bits transmitted from the BS to the MU and the expected energy cost, respectively. Under the HO and BT actions, we have that $r(u, a) = 0$ (since no bits are transmitted in these actions). On the other hand, under the DT action $a = (\text{DT}, \{\hat{s}\}, \text{SNR}, T_{\text{DT}})$ taken in slot k , the expected throughput in the t th communication slot, $t \in \{0, \dots, T_{\text{DT}} - 2\}$, is $\mathcal{T}^*(\text{SNR})$ as in (23), maximized over ϵ , if the current state is such that $S_{k+t}=\hat{s}$ and $B_{k+t}^{(I)} = 1$ (i.e., active beam in \hat{s}); otherwise, outage occurs and the expected throughput is zero. Therefore, $r(u, a)$ can be expressed as

$$\begin{aligned}
& r((s, I, b_1, b_2), (\text{DT}, \{\hat{s}\}, \text{SNR}, T_{\text{DT}})) \\
&= \mathcal{T}^*(\text{SNR}) \sum_{t=0}^{T_{\text{DT}}-2} \mathbb{P}(S_{k+t}=\hat{s}, B_{k+t}^{(I)}=1 | S_k=s, B_k^{(I)}=b_I) \\
&= \mathcal{T}^*(\text{SNR}) \sum_{t=0}^{T_{\text{DT}}-2} \mathbf{S}_{s \hat{s}}(t) \mathbf{B}_{b_I 1}^{(I)}(t). \quad (34)
\end{aligned}$$

The energy cost of an HO action is $e(u, a) = 0$; that of DT or BT action $a=(c, \hat{S}, \text{SNR}, T)$ is expressed from (9) as (note that $T = |\hat{S}|+1$ for a BT action and $|\hat{S}| = 1$ for a DT action)

$$e(u, a) = \frac{(T-1)\Delta_t}{|\hat{S}|} \sum_{\hat{s} \in \hat{\mathcal{S}}} \frac{\sigma_w^2}{\Upsilon_{\hat{s}}} \text{SNR}. \quad (35)$$

Note that the last slot of the DT or BT phases is reserved to the feedback transmission, with no energy cost for the BS.

Policy and Belief updates: Since the agent cannot directly observe the system state u_k , we define the *belief* $\beta \in \mathcal{B}$, i.e., the probability distribution over system states, given the information collected so far at the BS. Given β , the serving

BS selects an action a according to a policy $a = \pi(\beta)$, part of our design in Sec. IV; then upon executing the action a and receiving the feedback signal y , the BS updates the belief for the next decision interval according to Bayes' rule as

$$\beta'(u') = \mathbb{P}(u' | y, a, \beta) = \frac{\sum_{u \in \mathcal{U}} \mathbb{P}(u', y | u, a) \beta(u)}{\sum_{u \in \mathcal{U}} \sum_{u'' \in \mathcal{U}} \mathbb{P}(u'', y | u, a) \beta(u)}, \quad (36)$$

with $\mathbb{P}(u', y | u, a) \triangleq \mathbb{P}(U_{k+T}=u', Y_k=y | U_k=u, A_k=a)$ given by (31)-(28). We denote the belief update as $\beta' = \mathbb{B}(y, a, \beta)$.

IV. OPTIMIZATION PROBLEM

Our goal is to determine a policy π (i.e., a map from beliefs to actions) that maximizes the expected throughput, under an average power constraint \bar{P}_{avg} . Using Little's Theorem [23], the average rate and power consumption are, respectively, expressed as

$$\bar{T}^\pi \triangleq \frac{\bar{R}_{\text{tot}}^\pi}{D_{\text{tot}}}, \quad \bar{P}^\pi \triangleq \frac{\bar{E}_{\text{tot}}^\pi}{D_{\text{tot}}}, \quad (37)$$

where $\bar{R}_{\text{tot}}^\pi, \bar{E}_{\text{tot}}^\pi$ are the total expected number of bits transmitted and energy cost during an episode; D_{tot} is the expected episode duration, which only depends on the mobility process but is independent of the policy π . Therefore, we aim to solve

$$\begin{aligned}
& \max_{\pi} \bar{R}_{\text{tot}}^\pi \triangleq \mathbb{E}_{\pi} \left[\sum_{t=0}^{\infty} r(u_t, a_t) \middle| \beta_0 = \bar{\beta}_0^* \right], \quad (38) \\
& \text{s.t. } \bar{E}_{\text{tot}}^\pi \triangleq \mathbb{E}_{\pi} \left[\sum_{t=0}^{\infty} e(u_t, a_t) \middle| \beta_0 = \bar{\beta}_0^* \right] \leq \bar{D}_{\text{tot}} \bar{P}_{\text{avg}} = E_{\text{max}},
\end{aligned}$$

where $\bar{\beta}_0^*$ is the initial belief. We opt for a Lagrangian relaxation to handle the cost constraint, and define $\mathcal{L}_\lambda(u, a) = r(u, a) - \lambda e(u, a)$ for $\lambda \geq 0$. For a generic policy π , we define its value function as²

$$V_\lambda^\pi(\beta) = \mathbb{E}_{\pi} \left[\sum_{t=0}^{\infty} \mathcal{L}_\lambda(u_t, a_t) \middle| \beta_0 = \beta \right]. \quad (39)$$

The goal is to determine the optimal policy π^* which maximizes the value function, i.e.,

$$V_\lambda^*(\beta) \triangleq \max_{\pi} V_\lambda^\pi(\beta). \quad (40)$$

The optimal dual variable is then found via the dual problem

$$\lambda^* = \arg \min_{\lambda \geq 0} V_\lambda^*(\bar{\beta}_0^*) + \lambda E_{\text{max}}. \quad (41)$$

It is well known that the optimal value function for a given λ uniquely satisfies Bellman's optimality equation [2] $V_\lambda^* = H_\lambda[V_\lambda^*]$, where we have defined the operator $\hat{V} = H_\lambda[V]$ as

$$\hat{V}(\beta) = \max_{a \in \mathcal{A}} \sum_{u \in \mathcal{U}} \beta(u) \left[\mathcal{L}_\lambda(u, a) + \sum_{y, u'} \mathbb{P}(u', y | u, a) V(\mathbb{B}(y, a, \beta)) \right], \quad (42)$$

²Note that the convergence of this series is guaranteed by the presence of the absorbing state \bar{s} .

$\forall \beta \in \mathcal{B}$. The optimal value function V_λ^* can be arbitrarily well approximated via the value iteration algorithm $V_{n+1} = H_\lambda[V_n]$, where $V_0(\beta) = 0, \forall \beta$. Moreover, V_n is a piece-wise linear and concave function [2], so that, at any stage of the value iteration algorithm, it can be expressed by a finite set of hyperplanes $\mathcal{Q}_n \equiv \{(\alpha_{n,i}^{(r)}, \alpha_{n,i}^{(e)})\}_{i=1}^{A_n}$ of cardinality A_n , such that

$$V_n(\beta) = \max_{\alpha \in \mathcal{Q}_n} \beta \cdot (\alpha^{(r)} - \lambda \alpha^{(e)}), \quad (43)$$

where $\beta \cdot \alpha = \sum_u \beta(u) \alpha(u)$ denotes inner product. Each hyperplane $(\alpha^{(r)}, \alpha^{(e)}) \in \mathcal{Q}_n$ is associated with an action $a_\alpha \in \mathcal{A}$, so that the maximizing hyperplane α^* in (43) defines the policy $\pi_n(b) = a_{\alpha^*}$. Note that a distinguishing feature of our approach compared to [2] is that we define distinct hyperplanes $\alpha^{(r)}$ for the reward and $\alpha^{(e)}$ for the cost; as we will see later, this approach allows to more efficiently track changes in the dual variable λ , as part of the dual problem (41), and to compute the expected total reward and cost as

$$\begin{aligned} \bar{R}_n(\beta) &= \beta \cdot \alpha^{(r)*}, \quad \bar{E}_n(\beta) = \beta \cdot \alpha^{(e)*}, \\ \text{where } (\alpha^{(r)*}, \alpha^{(e)*}) &= \arg \max_{\alpha \in \mathcal{Q}_n} \beta \cdot (\alpha^{(r)} - \lambda \alpha^{(e)}). \end{aligned} \quad (44)$$

It can be shown (see for instance [24]) that the set of hyperplanes is updated recursively as

$$\begin{aligned} \mathcal{Q}_{n+1} \equiv & \left\{ (r(\cdot, a), e(\cdot, a)) + \sum_{\hat{u}, y} \mathbb{P}(\hat{u}, y | \cdot, a) (\alpha_y^{(r)}(\hat{u}), \alpha_y^{(e)}(\hat{u})): \right. \\ & \left. a \in \mathcal{A}, [(\alpha_y^{(r)}, \alpha_y^{(e)})]_{\forall y \in \mathcal{Y}} \in \mathcal{Q}_n^{|\mathcal{Y}|} \right\}, \end{aligned} \quad (45)$$

so that the cardinality grows as $A_{n+1} = |\mathcal{Q}_{n+1}| = A_n^{|\mathcal{Y}|} |\mathcal{A}| = |\mathcal{A}|^{|\mathcal{Y}|^n}$ – doubly exponentially with the number of iterations. For this reason, computing optimal planning solutions for POMDPs is an intractable problem for any reasonably sized task. This calls for approximate solution techniques, e.g., PERSEUS [2], which we introduce next.

PERSEUS [2] is an approximate PBVI algorithm for POMDPs. Its key idea is to define an approximate backup operator $\tilde{H}_\lambda[\cdot]$ (in place of $H_\lambda[\cdot]$), restricted to a discrete subset of belief points in $\tilde{\mathcal{B}}$, chosen as representative of the entire belief space \mathcal{B} ; in other words, for a given value function \tilde{V}_n at stage n , PERSEUS builds a value function $\tilde{V}_{n+1} = \tilde{H}[\tilde{V}_n]$ that improves the value of all belief points $\beta \in \tilde{\mathcal{B}}$, without regard for the belief points outside of this discrete set, $\beta \notin \tilde{\mathcal{B}}$. The goal of the algorithm is to provide a $|\tilde{\mathcal{B}}|$ -dimensional set of hyperplanes $\alpha = (\alpha^{(r)}, \alpha^{(e)}) \in \mathcal{Q}$ and associated actions a_α . Given such set, the value function at any other belief point $\beta \in \mathcal{B}$ is then approximated via (43) as $\tilde{V}(\beta) = \beta \cdot (\alpha^{(r)} - \lambda \alpha^{(e)})^*$, where $\alpha^* = (\alpha^{(r)}, \alpha^{(e)})^* = \arg \max_{(\alpha^{(r)}, \alpha^{(e)}) \in \mathcal{Q}} \beta \cdot (\alpha^{(r)} - \lambda \alpha^{(e)})$, which defines an approximately optimal policy $\pi(\beta) = a_{\alpha^*}$.

The approximate backup operation of PERSEUS is given by Algorithm 1, which takes as input a set of hyperplanes \mathcal{Q}_n and the corresponding actions, and outputs a new set \mathcal{Q}_{n+1} along with their corresponding actions. To do so: in line 4, a belief point is chosen randomly from $\tilde{\mathcal{B}}_{\text{temp}}$; in lines 5-7, the hyperplane associated with each action $a \in \mathcal{A}$ is computed; in particular, line 6 computes the hyperplane associated with the future value function $V_n(\mathbb{B}(y, a, \beta))$, for each possible observation y resulting in the belief update $\mathbb{B}(y, a, \beta)$; line 7 instead performs the backup operation to determine the new hyper-

Algorithm 1: function PERSEUS

```

input :  $\lambda, \tilde{\mathcal{B}}, \mathcal{Q}_n, \{a_\alpha^n, \alpha \in \mathcal{Q}_n\}$ 
1 Init:  $\tilde{V}_{n+1}(\tilde{\beta}) = -\infty, \forall \tilde{\beta} \in \tilde{\mathcal{B}}; \tilde{\mathcal{B}}_{\text{temp}} \equiv \tilde{\mathcal{B}}, \mathcal{Q}_{n+1} = \emptyset$ 
2  $\tilde{V}_n(\tilde{\beta}) \leftarrow \max_{\alpha \in \mathcal{Q}_n} \tilde{\beta} \cdot (\alpha^{(r)} - \lambda \alpha^{(e)})$ , and maximizer
    $(\alpha_{\tilde{\beta}}^{(r)}, \alpha_{\tilde{\beta}}^{(e)}), \forall \tilde{\beta} \in \tilde{\mathcal{B}}$ 
3 while  $\tilde{\mathcal{B}}_{\text{temp}} \neq \emptyset$  do // Unimproved beliefs
4   Sample  $\beta$  from  $\tilde{\mathcal{B}}_{\text{temp}}$  (e.g., uniformly)
5   for each action  $a$  do
6      $\alpha_{y,a}^* = \arg \max_{\alpha \in \mathcal{Q}_n} \mathbb{B}(y, a, \beta) \cdot (\alpha^{(r)} - \lambda \alpha^{(e)}), \forall y \in \mathcal{Y}$ 
7      $\hat{\alpha}_a^* = (r(\cdot, a), e(\cdot, a)) + \sum_{\hat{u}, y} \mathbb{P}(\hat{u}, y | \cdot, a) (\alpha_{y,a}^{*(r)}(\hat{u}), \alpha_{y,a}^{*(e)}(\hat{u}))$ 
8   Solve  $V_{n+1}(\beta) = \max_{a \in \mathcal{A}} \beta \cdot (\hat{\alpha}_a^{*(r)} - \lambda \hat{\alpha}_a^{*(e)})$  and
     maximizing action  $a^*$  and  $\hat{\alpha} = \hat{\alpha}_{a^*}$ 
9   if  $V_{n+1}(\beta) > \tilde{V}_n(\beta)$  then //  $\hat{\alpha}$  improves value
10     $\mathcal{Q}_{n+1} \leftarrow \mathcal{Q}_{n+1} \cup \{\hat{\alpha}\}; a_{\hat{\alpha}}^{n+1} = a^*$  // add  $\hat{\alpha}$  to
      $\mathcal{Q}_{n+1}$  and define action associated with  $\hat{\alpha}$ ;
11  else // keep previous hyperplane  $\alpha_\beta$ 
12     $\hat{\alpha} = \alpha_\beta; \mathcal{Q}_{n+1} \leftarrow \mathcal{Q}_{n+1} \cup \{\alpha_\beta\}; a_{\alpha_\beta}^{n+1} = a_{\alpha_\beta}^n$ 
13   $\tilde{V}_{n+1}(\tilde{\beta}) \leftarrow \max\{\tilde{\beta} \cdot (\hat{\alpha}^{(r)} - \lambda \hat{\alpha}^{(e)}), \tilde{V}_n(\tilde{\beta})\}, \forall \tilde{\beta} \in \tilde{\mathcal{B}}$ 
14   $\tilde{\mathcal{B}}_{\text{temp}} \leftarrow \{\tilde{\beta} \in \tilde{\mathcal{B}}_{\text{temp}}: \tilde{V}_{n+1}(\tilde{\beta}) < \tilde{V}_n(\tilde{\beta})\}$  // New set of
     unimproved beliefs
15 return  $\mathcal{Q}_{n+1}, \{a_\alpha^{n+1}, \forall \alpha \in \mathcal{Q}_{n+1}\}$  // new hyperplanes
     and associated actions

```

plane of $V_{n+1}(\beta)$ associated to action a ; line 8 determines the optimal action that maximizes the value function, so that lines 5-8 yield overall the value iteration update $V_{n+1}(\beta) = \max_a \mathbb{E}_{U, Y | a, \beta} [r(U, a) - \lambda e(U, a) + V_n(\mathbb{B}(Y, a, \beta))]$; in lines 9-12, the new hyperplane and the associated action is added to the set \mathcal{Q}_{n+1} , but only if it yields an improvement in the value function $V_{n+1}(\beta) > \tilde{V}_n(\beta)$; otherwise, the previous hyperplane is used; finally, lines 13-14 update the set of unimproved belief based on the newly added hyperplane; only the belief points that have not been improved are part of the next iterations of the algorithm, until all beliefs have been improved (empty $\tilde{\mathcal{B}}_{\text{temp}}$). Overall, the algorithm guarantees monotonic improvements of the value function in \mathcal{B} .

Key to the performance of PERSEUS is the design of $\tilde{\mathcal{B}}$, which should be representative of the beliefs encountered in the system dynamics. In the PBVI literature [24], most of the strategies to design $\tilde{\mathcal{B}}$ focus on selecting reachable belief points, rather than covering uniformly the entire belief simplex. We choose the belief points in the following two steps. An initial belief points set \mathcal{B}_0 is selected deterministically to cover uniformly the belief space, followed by expansion of \mathcal{B}_0 using the *Stochastic simulation and exploratory action* (SSEA) algorithm [24] to yield the expanded belief points set $\tilde{\mathcal{B}}$. After initializing \mathcal{B}_0 , given \mathcal{B}_n at iteration n , for each $\beta \in \mathcal{B}_n$, SSEA performs a one step forward simulation with each action in the action set, thus producing new beliefs $\{\beta_a, \forall a \in \mathcal{A}\}$. At this point, it computes the L1 distance between each new β_a and its closest neighbor in \mathcal{B}_n , and adds the point β_{a^*} farthest away from \mathcal{B}_n , so as to more widely cover the belief space. This expansion is performed multiple times to obtain $\tilde{\mathcal{B}}$.

The basic routine for PBVI is given in Algorithm 2. However, differently from [2], we also embed the dual optimization

Algorithm 2: Point-Based Value Iteration (PBVI) with embedded dual optimization

1 **Init:** belief set $\tilde{\mathcal{B}}$; hyperplanes $\mathcal{Q}_0 = \{(\mathbf{0}, \mathbf{0})\}$; optimal actions $a_{(0,0)}^0 = \text{HO}$; value function $V_{n+1}(\beta) = 0, \forall \beta \in \tilde{\mathcal{B}}$; $\lambda_0 \geq 0$; stepsize $\{\gamma_n = \gamma_0 / (n + 1), n \geq 0\}$

2 **for** $n = 0, \dots$ **do**

3 $(\mathcal{Q}_{n+1}, \{a_\alpha^{n+1}, \forall \alpha \in \mathcal{Q}_{n+1}\}) =$
PERSEUS $(\lambda_n, \tilde{\mathcal{B}}, \mathcal{Q}_n, \{a_\alpha^n, \alpha \in \mathcal{Q}_n\})$

4 $V_{n+1}(\beta) = \max_{\alpha \in \mathcal{Q}_{n+1}} \beta \cdot (\alpha^{(r)} - \lambda_n \alpha^{(e)}), \forall \beta \in \tilde{\mathcal{B}}$

5 Let $\bar{E}_{n+1} = \tilde{\beta}_0^* \cdot \alpha_{\beta_0^*}^{(e)*}$, where
 $\alpha^* = \arg \max_{\alpha \in \mathcal{Q}_{n+1}} \tilde{\beta}_0^* \cdot (\alpha^{(r)} - \lambda_n \alpha^{(e)})$

6 $\lambda_{n+1} = \max\{\lambda_n + \gamma_n (\bar{E}_{n+1} - E_{\max}), 0\}$

7 **if** $\max_{\beta \in \tilde{\mathcal{B}}} |V_{n+1}(\beta) - V_n(\beta)| < \epsilon_V$, $\bar{E}_{n+1} \leq E_{\max}$
and $\lambda_n |\bar{E}_{n+1} - E_{\max}| < \epsilon_E$ **then**

8 **return** $\mathcal{Q}_{n+1}, \{a_\alpha^{n+1}, \forall \alpha \in \mathcal{Q}_{n+1}\}, \lambda_n$

(41) by updating the dual variable λ in line 6. In line 3, we perform one backup operation via PERSEUS (Algorithm 1); in line 4, we compute the new value function $V_{n+1}(\beta)$ (based on the new hyperplane set \mathcal{Q}_{n+1}); in line 5, we compute the approximate cost \bar{E}_{n+1} starting from the initial belief $\tilde{\beta}_0^*$, based on the optimal hyperplane α^* ; this is used in line 6 to update the dual variable λ via projected subgradient descent, with the goal to solve the dual problem (41) (note that $E_{\max} - \bar{E}_{n+1}$ is a subgradient of the dual function, see [25]): as a result, λ_n is decreased if the estimated cost $\bar{E}_{n+1} < E_{\max}$, to promote throughput maximization over energy cost minimization, otherwise it is increased; the algorithm continues until the KKT conditions are approximately satisfied [25], i.e., $\max_{\beta \in \tilde{\mathcal{B}}} |V_{n+1}(\beta) - V_n(\beta)| < \epsilon_V$ (i.e., an approximately fixed point of $V_{n+1} = \tilde{H}[V_n]$ has been determined and PERSEUS converged), $\bar{E}_{n+1} \leq E_{\max}$ (primal feasibility constraint satisfied) and $\lambda_n |\bar{E}_{n+1} - E_{\max}| < \epsilon_{CS}$ (complementary slackness; note that dual feasibility $\lambda_n \geq 0$ is enforced automatically in line 6).

After returning the set of hyperplanes \mathcal{Q}_{n+1} , the associated actions $\{a_\alpha^{n+1}, \forall \alpha \in \mathcal{Q}_{n+1}\}$, and the dual variable λ_n , the (approximately) optimal action to be selected when operating under the belief β can be computed as

$$\pi^*(\beta) = a_{\alpha^*}^{n+1}, \text{ where } \alpha^* = \arg \max_{\alpha \in \mathcal{Q}_{n+1}} \beta \cdot (\alpha^{(r)} - \lambda_n \alpha^{(e)}),$$

along with the approximate expected reward and cost via (44).

In Fig. 2, we plot a time-series of the following variables for a portion of an episode executed under the PERSEUS-based policy (Algorithms 1 and 2): sector index S_k , index of the serving BS I_k , its blockage state $B_k^{(I_k)}$, the action class $c \in \{\text{DT}, \text{BT}, \text{HO}\}$, the BT and DT feedbacks Y_{BT} and Y_{DT} as defined in (13) and (24). The simulation parameters are listed in Table 1. Initially, the MU is known to be in sector $S_0=1$, with LOS conditions for both BSs ($B_0^{(1)}=B_0^{(2)}=1$). It can be observed in the figure that at 0.238s, 0.246s and 0.287s, NACKs ($Y_{\text{DT}} = \emptyset$) are received after executing the DT action. After each one of these NACKs, the policy executes the BT action. If the BT feedback $Y_{\text{BT}} \neq \emptyset$, then DT is performed;

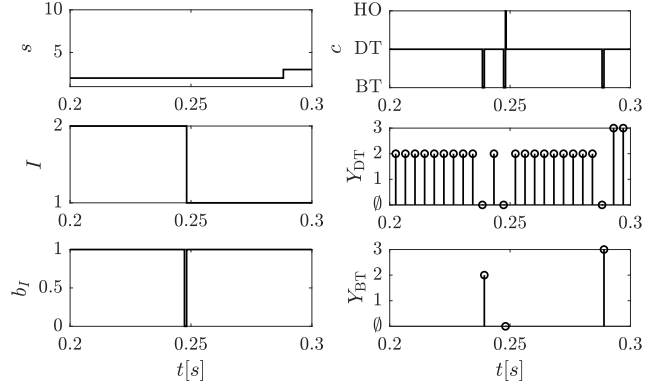


Fig. 2: Execution of policy π^* .

otherwise, blockage is detected and the HO action is executed.

It should be noted that, although Algorithm 2 returns an approximately optimal design, it incurs a huge computational cost in POMDPs with large state and action spaces (hence large number of representative belief points). To remedy this, in the subsequent section we propose simple heuristic policies, inspired by the behavior of the PERSEUS-based policy described earlier and depicted in Fig. 2. These policies will be shown numerically to achieve *near-optimal* performance.

V. HEURISTIC POLICIES

In this section, we present two heuristic policies, namely a belief-based heuristic (B-HEU) and a finite-state-machine (FSM)-based heuristic (FSM-HEU) and present closed-form expressions for the performance of FSM-HEU. Similarly to PERSEUS-based, B-HEU needs to track the belief β , whereas FSM-HEU is solely based on the current observation signal that defines transitions in a FSM. For this reason, FSM-HEU has lower complexity than B-HEU, while achieving only a small degradation in performance (see Sec. VI).

A. FSM-based Heuristic policy (FSM-HEU)

The key idea of FSM-HEU is that it selects actions based solely on a FSM, whose states define the action to be selected, and whose transitions are defined by the observation signal, as depicted in Fig. 3 and described next. In FSM-HEU, we consider the following actions:

- the HO action $A_k = (\text{HO}, \emptyset, 0, T_{\text{HO}})$ of duration T_{HO} ;
- the BT action $A_k = (\text{BT}, \mathcal{S}, \text{SNR}_{\text{BT}}, T_{\text{BT}})$ of duration $T_{\text{BT}} = |\mathcal{S}| + 1$; in other words, the serving BS performs an exhaustive search, with a fixed SNR SNR_{BT} (determined offline), followed by feedback;
- the $|\mathcal{S}|$ DT actions $(\text{DT}, \hat{s}, \text{SNR}_{\text{DT}}, T_{\text{DT}})$, where $\hat{s} \in \mathcal{S}$; in other words, the serving BS performs DT with fixed SNR SNR_{DT} and duration T_{DT} (both determined offline).

For notational convenience, we compactly refer to these actions as HO, BT and (DT, \hat{s}) , $\hat{s} \in \mathcal{S}$, respectively. Let $A_k \in \{\text{BT}, \text{HO}\} \cup \{(\text{DT}, \hat{s}) : \hat{s} \in \mathcal{S}\}$ be the selected action (the state of the FSM at time k), of duration T , and Y_k be the observation signal generated by such action, as described in Sec. III; then, the FSM moves to state $A_{k+T} = \mathbb{A}(A_k, Y_k)$, which defines the next action A_{k+T} to be selected in the next decision round. Note that \mathbb{A} defines transitions in the FSM, and the process continues until the episode terminates.

Let us consider the transitions in the FSM, defined by the function \mathbb{A} , depicted in Fig. 3. If $A_k = \text{BT}$ and the observation

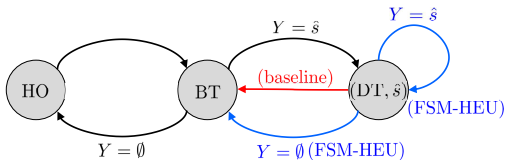


Fig. 3: Evolution of the selected action A_k based on the observation signal Y_k . Black lines represent the transitions under both FSM-HEU and baseline policies; blue lines represent transitions under the FSM-HEU policy only; the red line represents the transition under the baseline policy only.

signal is $Y_k=(I, \hat{s})$, $\hat{s} \in \mathcal{S}$, then the BS detects the strongest beam \hat{s} ; hence FSM-HEU switches to DT and uses the DT action $A_{k+T}=(DT, \hat{s})=\mathbb{A}(BT, \hat{s})$ in the next decision round, of duration T_{DT} . On the other hand, if the observation signal is $Y_k=\emptyset$, the BS detects blockage and performs HO to the non-serving BS, so that the new action is $A_{k+T}=\text{HO}=\mathbb{A}(BT, \emptyset)$.

If $A_k=(DT, \hat{s})$, i.e., the DT action is executed on sector \hat{s} , of duration T_{DT} , and the signal $Y_k=\hat{s}$ is observed, then the BS infers that the signal is still sufficiently strong to continue DT on the same sector, and the same action $A_{k+T}=(DT, \hat{s})=\mathbb{A}((DT, \hat{s}), \hat{s})$ is selected again. Otherwise ($Y_k=\emptyset$), the BS detects a loss of alignment, hence the BT action $A_{k+T}=\text{BT}=\mathbb{A}((DT, \hat{s}), \emptyset)$ is executed next.

Finally, if $A_k=\text{HO}$ (the HO action is chosen, with observation signal $Y_k=\emptyset$), then the new serving BS executes the BT action $A_{k+T}=\text{BT}=\mathbb{A}(\text{HO}, \emptyset)$ next. This procedure continues until the episode terminates.

The performance of FSM-HEU can be computed in closed form by noticing that $G_k=(U_k, A_k)$, i.e., the underlying system state U_k and action A_k , form a Markov chain, taking values from the state space

$$\mathcal{G} \equiv \mathcal{U} \times [\{\text{BT}, \text{HO}\} \cup \{(\text{DT}, \hat{s}) : \hat{s} \in \mathcal{S}\}].$$

To see this, note that the observation Y_k and next state U_{k+T} (where T is the duration of the selected action A_k) have joint distribution given by (32)-(28), which solely depends on G_k ; then, in view of the FSM of Fig. 3, $A_{k+T} = \mathbb{A}(A_k, Y_k)$ is a deterministic function of A_k and Y_k . The state transition probability is then obtained by computing the marginal with respect to the observation signal Y_k , yielding

$$\begin{aligned} \mathbb{P}(G'_{k+T} = (s', I', b'_1, b'_2, a') | G_k = (s, I, b_1, b_2, a)) \\ = \sum_{y \in \mathcal{Y}: \mathbb{A}(a, y) = a'} \mathbb{P}(U_{k+T} = (s', I', b'_1, b'_2), Y_k = y | U_k = (s, I, b_1, b_2), A_k = a). \end{aligned} \quad (46)$$

We remind that the right hand side of (46) is given by (32)-(28). Let $\bar{R}_{\text{tot}}^{\text{FSM}}(g)$ and $\bar{E}_{\text{tot}}^{\text{FSM}}(g)$ be the total expected number of bits delivered and energy cost under FSM-HEU, starting from state g . Then, with $\mathbb{P}(g'|g)$ defined in (46) and $g = (u, a)$,

$$\begin{aligned} \bar{R}_{\text{tot}}^{\text{FSM}}(u, a) &= r(u, a) + \sum_{(u', a') \in \mathcal{G}} \mathbb{P}(u', a' | u, a) \bar{R}_{\text{tot}}^{\text{FSM}}(u', a'), \\ \bar{E}_{\text{tot}}^{\text{FSM}}(u, a) &= e(u, a) + \sum_{(u', a') \in \mathcal{G}} \mathbb{P}(u', a' | u, a) \bar{E}_{\text{tot}}^{\text{FSM}}(u', a'), \end{aligned}$$

where $r(\cdot)$ and $e(\cdot)$ are given by (34)-(35). We can solve these equations in closed form, yielding

$$\bar{\mathbf{R}}_{\text{tot}}^{\text{FSM}} = (\mathbf{I} - \mathbf{P}^{\text{FSM}})^{-1} \mathbf{r}, \quad \bar{\mathbf{E}}_{\text{tot}}^{\text{FSM}} = (\mathbf{I} - \mathbf{P}^{\text{FSM}})^{-1} \mathbf{e}, \quad (47)$$

where $\bar{\mathbf{R}}_{\text{tot}}^{\text{FSM}} = [\bar{R}_{\text{tot}}^{\text{FSM}}(g)]_{g \in \mathcal{G}}$, $\bar{\mathbf{E}}_{\text{tot}}^{\text{FSM}} = [\bar{E}_{\text{tot}}^{\text{FSM}}(g)]_{g \in \mathcal{G}}$, $\mathbf{r} = [r(g)]_{g \in \mathcal{G}}$, $\mathbf{e} = [e(g)]_{g \in \mathcal{G}}$, $[\mathbf{P}^{\text{FSM}}]_{g, g'} = \mathbb{P}(g'|g)$.

Parameter	Symbol	Value
Number of BS antennas	M_{tx}	128
Angular BS coverage	Θ	90°
Slot duration	Δ_t	$100 \mu\text{s}$
Distance of road to BS	D	20m
Number of Sectors	S	9
Bandwidth	W_{tot}	100MHz
Carrier frequency	f_c	30GHz
Noise psd	N_0	-174dBm/Hz
Noise figure	F	10dB
Sidelobe/mainlobe SNR ratio	ρ	-22dB
Fraction of DT slot for channel estimation	κ	0.01
HO delay	T_{HO}	1 slot
TX power	$P_{\text{BT}}, P_{\text{DT}}$	{0, 10, 20, 30, 40}dBm
DT duration	T_{DT}	{10, 20, 40} slots
Steady state blockage prob.	$\pi_0^{(1)}, \pi_0^{(2)}$	0.2
Avg blockage duration	$D_B^{(1)}, D_B^{(2)}$	0.2ms
MU average speed	μ_v	30m/s
MU speed st. dev.	σ_v	10
MU mobility memory param.	γ	0.2
Accuracy for Algorithm 2	ϵ_C, ϵ_V	0.01
B-HEU threshold	(η_1, η_2, η_3)	(0.1, 0.8, 0.95)

TABLE 1: Simulation parameters.

B. Belief-based Heuristic policy (B-HEU)

Differently from FSM-HEU, this policy exploits the belief β_k in the decision-making process. However, B-HEU selects actions in a heuristic fashion as described next, as opposed to PERSEUS-based (Algorithm 1), which selects actions (approximately) optimally. To describe this policy, let β be the current belief and I be the index of the serving BS. Let $\Xi(s) \triangleq \sum_{(b_1, b_2): b_I=1} \beta(s, I, b_1, b_2)$ be the marginal probability of the MU occupying sector s with no blockage under the serving BS. Then, $\Lambda \triangleq \sum_s \Xi(s)$ can be interpreted as the probability of no blockage under the serving BS. Given these quantities, B-HEU operates as follows, with thresholds η_1 , η_2 and η_3 determined offline: if $\Lambda < \eta_1$, then blockage is detected, hence the HO action is selected; otherwise ($\Lambda \geq \eta_1$), let $\hat{s}^* = \arg \max \Xi(s)$ be the sector most likely occupied by the MU: if $\Xi(\hat{s}^*) \geq \eta_2$, i.e., the BS is confident that the MU is in sector \hat{s}^* and there is no blockage, then the BS performs DT over sector \hat{s}^* , with SNR SNR_{DT} and duration T_{DT} determined offline. Otherwise ($\Lambda \geq \eta_1$ and $\Xi(\hat{s}^*) < \eta_2$), the BS is uncertain on the location of the BS, hence it performs BT over the most likely sectors in the set $\hat{\mathcal{S}}^*$ defined as

$$\hat{\mathcal{S}}^* \triangleq \arg \min_{\hat{\mathcal{S}} \subseteq \mathcal{S}} |\hat{\mathcal{S}}| \text{ s.t.: } \sum_{s \in \hat{\mathcal{S}}} \Xi(s) \geq \eta_3, \quad (48)$$

thus neglecting the least likely sectors whose aggregate probability is less than $1 - \eta_3$.

After selecting the appropriate action based on the belief, the serving BS collects the observation Y_k and updates its belief as in (36). Note that, unlike FSM-HEU which performs an exhaustive search during the BT phase, B-HEU exploits the current belief β to perform BT only on the most likely sectors, and therefore incurs less BT overhead.

VI. NUMERICAL RESULTS

In this section, we perform a numerical evaluation of the proposed policies. We also compare their performance with a baseline policy. The baseline policy is the same as FSM-HEU except for one key difference: after executing the DT action, it executes the BT action irrespective of the binary feedback. In other words, $\mathbb{A}((DT, \hat{s}), Y) = \text{BT}, \forall Y$. Note that, if no

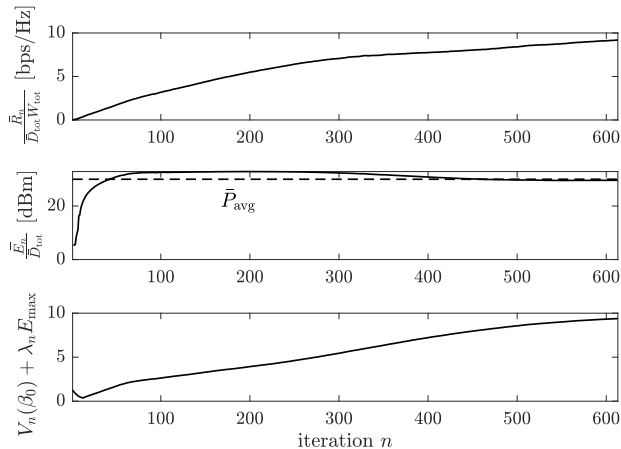


Fig. 4: Convergence of PBVI Algorithm 2.

blockage is detected, baseline mimics the periodic exhaustive search. Its performance can be analyzed in closed form in a similar fashion as for FSM-HEU (see its FSM representation in Fig. 3). The simulation parameters are listed in Table 1.

Using the throughput and power metrics defined in (37), the average spectral efficiency (bps/Hz) and power (dBm) under policy π are expressed as T^π / W_{tot} and P^π . We choose the initial belief $\beta_0^*(u) = \chi(u = u_0)$, where $u_0 = (1, 1, 1, 1)$, implying that the MU starts in sector $s=1$ with LOS conditions for both BS. We use the Gauss-Markov mobility model, with speed v_k and position x_k of the MU given by

$$v_k = \gamma v_{k-1} + (1 - \gamma)\mu_v + \sigma_v \sqrt{1 - \gamma^2} \tilde{v}_{k-1}, \quad (49)$$

$$x_k = x_{k-1} + \Delta_t v_{k-1}, \quad (50)$$

where, unless otherwise stated, $\mu_v = 30\text{m/s}$ is the average speed; $\sigma_v = 10\text{m/s}$ is the standard deviation of speed; $\gamma = 0.2$ is the memory parameter; $\tilde{v}_{k-1} \sim \mathcal{N}(0, 1)$, i.i.d. over slots. In the simulations, we show the results corresponding to the analytical model presented in the paper (with \mathbf{P} estimated from simulations of 10000 trajectories under the Gauss-Markov model (49), as described in Sec. II-A) as well as the results obtained through Monte-Carlo simulation using the beamformer design [22] and the Gauss-Markov mobility model.

In Fig. 4, we depict the convergence of the PBVI Algorithm 2, which optimizes both the policy π and the dual variable λ to meet the power constraint $P^\pi \leq \bar{P}_{avg}$. It can be observed that the expected spectral efficiency $\bar{R}_n / \bar{D}_{tot} / W_{tot}$, average power $\bar{E}_n / \bar{D}_{tot}$ and Lagrangian function $V_n(\beta_0) + \lambda_n E_{max}$ converge, and $\bar{E}_n / \bar{D}_{tot}$ converges to the desired average power constraint \bar{P}_{avg} .

In Fig. 5, we depict the average spectral efficiency against the average power consumption. For the heuristic policies, we set $T_{DT} = 10$ and $P_{BT} = P_{DT}$ is varied from 0dBm to 40dBm. The upper-bound shown in the figure is obtained by a genie-aided policy that always executes DT with perfect knowledge of the state (s, I, b_1, b_2) and hence its throughput performance can be upper bounded by $(1 - \pi_B^{(1)} \pi_B^{(2)})(1 - \kappa) \mathcal{T}^*(\text{SNR})$, whereas the power consumption is given as $(1 - \pi_B^{(1)} \pi_B^{(2)}) P_{DT}$, where $\pi_B^{(1)} \pi_B^{(2)}$ is the steady-state probability that both BSs are under blockage, resulting in outage. It should be noted that this upper-bound is loose since it is found by assuming the perfect knowledge of state and ignoring the performance degradation due to transitions in s during a DT action and time required

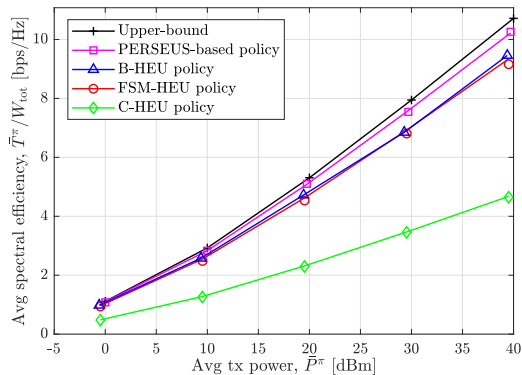


Fig. 5: Average spectral efficiency versus average power consumption. The continuous lines represent the analytical curves based on the sectorized model and synthetic mobility (generated based on the sector transition probability \mathbf{P}), whereas the markers represent the simulation using analog beamforming and actual mobility.

to perform handover and transmit feedback. The PERSEUS-based policy π^* yields the best performance with negligible performance gap with respect to the upper-bound. It shows a performance gain of up to 10%, 11% and 55% compared to B-HEU, FSM-HEU and baseline, respectively. It is also observed that B-HEU and FSM-HEU yield similar performance. On the other hand, the baseline scheme yields up to 50% degraded performance compared to the proposed adaptive schemes: in fact, it neglects the DT feedback and instead performs periodic BT, thus incurring significant overhead. We observe that the curves corresponding to analysis and the markers, representing simulation points obtained considering analog beam design and Gauss Markov mobility, closely match, thereby demonstrating the accuracy of the model introduced in the paper to model more realistic settings.

In Fig. 6, the spectral efficiency is depicted against the DT time duration T_{DT} used in B-HEU, FSM-HEU and baseline schemes. As observed previously, the PERSEUS-based policy outperforms B-HEU and FSM-HEU, and all of them outperform the baseline scheme. B-HEU and FSM-HEU show similar performance, and achieve near-optimal performance with an optimized value of $T_{DT} \simeq 60[\text{slots}]$. Most remarkably, this near-optimal performance is achieved at a fraction of the complexity of PERSEUS-based. It is observed that the spectral efficiency initially improves by increasing the T_{DT} due to reduced overhead of BT and feedback time. However, after achieving a maximum value at $T_{DT} \simeq 60[\text{slots}]$, the spectral efficiency decreases as T_{DT} is further increased. This is attributed to the fact that during very large data transmission periods, loss of alignment and blockages are more likely to occur before the serving BS is able to react to these events. It is also observed that the baseline scheme achieves peak performance at a much higher value of $T_{DT} \simeq 180[\text{slots}]$. In fact, since baseline performs periodic BT, there is a stronger incentive to reduce the overhead by extending the duration of DT, as opposed to B-HEU and FSM-HEU which adapt the duration of DT based on the DT feedback signal.

In Fig. 7, we demonstrate the impact of the mobility process on the performance, by plotting the total expected number of bits delivered successfully under FSM-HEU and baseline versus the average speed μ_v , for different values of σ_v . In the figure, it can be observed that, as the average speed increases, the performance degrades due to an increase in frequency of

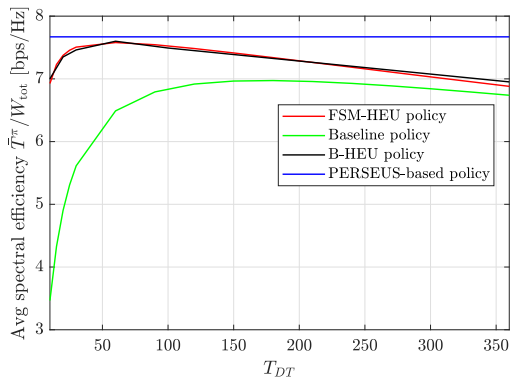


Fig. 6: Average spectral efficiency versus T_{DT} ; $P_{BT} = P_{DT} = 30\text{dBm}$.

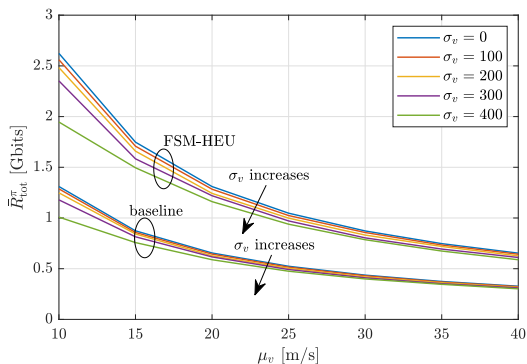


Fig. 7: Average data transferred versus mean speed for different values of σ_v ; $P_{BT} = P_{DT} = 30\text{dBm}$, $T_{DT} = 10$.

mis-alignments as well as due to a shorter episode duration. On the other hand, the performance loss due to variations in the speed is only significant at very high values of σ_v , showing that the proposed heuristic policies are robust to variations in speed. As previously observed, the FSM-HEU outperforms baseline in all range of values considered.

VII. CONCLUSIONS

In this paper, we investigated the design of beam-training/data-transmission/handover strategies for mm-wave vehicular networks. The mobility and blockage dynamics have been leveraged to obtain the approximately optimal policy via a POMDP formulation and its solution via a point-based value iteration (PBVI) algorithm based on a variation of PERSEUS [2]. Our numerical results demonstrate superior performance of the PERSEUS-based policy compared to a baseline scheme with periodic beam training (up to $2\times$ improvement in spectral efficiency). Inspired by the behavior of the PERSEUS-based policy, we proposed two heuristic policies, which provide low computational alternatives to PBVI and exhibit near-optimal performance (within $\sim 10\%$).

REFERENCES

- [1] M. Hussain, M. Scalabrin, M. Rossi, and N. Michelusi, "Adaptive millimeter-wave communications exploiting mobility and blockage dynamics," 2019, submitted to IEEE ICC 2020. [Online]. Available: <https://engineering.purdue.edu/~michelus/icc2020.pdf>
- [2] M. T. J. Spaan and N. Vlassis, "Perseus: Randomized point-based value iteration for pomdps," *J. Artif. Int. Res.*, vol. 24, no. 1, pp. 195–220, Aug. 2005.
- [3] J. Choi, V. Va, N. Gonzalez-Prelcic, R. Daniels, C. R. Bhat, and R. W. Heath, "Millimeter-wave vehicular communication to support massive automotive sensing," *IEEE Communications Magazine*, vol. 54, no. 12, pp. 160–167, 2016.

- [4] N. Michelusi and M. Hussain, "Optimal beam-sweeping and communication in mobile millimeter-wave networks," in *2018 IEEE International Conference on Communications (ICC)*, May 2018, pp. 1–6.
- [5] Z. Marzi, D. Ramasamy, and U. Madhoo, "Compressive channel estimation and tracking for large arrays in mm-wave picocells," *IEEE Journal of Selected Topics in Signal Processing*, vol. 10, no. 3, pp. 514–527, April 2016.
- [6] V. Va, J. Choi, T. Shimizu, G. Bansal, and R. W. Heath, "Inverse multipath fingerprinting for millimeter wave v2i beam alignment," *IEEE Transactions on Vehicular Technology*, vol. 67, no. 5, pp. 4042–4058, May 2018.
- [7] M. Giordani, M. Mezzavilla, and M. Zorzi, "Initial access in 5g mmwave cellular networks," *IEEE Communications Magazine*, vol. 54, no. 11, pp. 40–47, November 2016.
- [8] V. Va, T. Shimizu, G. Bansal, and R. W. Heath, "Beam design for beam switching based millimeter wave vehicle-to-infrastructure communications," in *2016 IEEE ICC*, 2016, pp. 1–6.
- [9] M. Scalabrin, N. Michelusi, and M. Rossi, "Beam training and data transmission optimization in millimeter-wave vehicular networks," in *2018 IEEE Globecom*, Dec 2018, pp. 1–7.
- [10] M. Mezzavilla, S. Goyal, S. Panwar, S. Rangan, and M. Zorzi, "An mdp model for optimal handover decisions in mmwave cellular networks," in *Networks and Communications (EuCNC), 2016 European Conference on*. IEEE, 2016, pp. 100–105.
- [11] J. Pan and W. Zhang, "An mdp-based handover decision algorithm in hierarchical lte networks," in *Vehicular Technology Conference (VTC Fall), 2012 IEEE*. IEEE, 2012, pp. 1–5.
- [12] E. Stevens-Navarro, Y. Lin, and V. W. Wong, "An mdp-based vertical handoff decision algorithm for heterogeneous wireless networks," *IEEE Transactions on Vehicular Technology*, vol. 57, no. 2, pp. 1243–1254, 2008.
- [13] A. Alkhateeb, S. Alex, P. Varkey, Y. Li, Q. Qu, and D. Tujkovic, "Deep learning coordinated beamforming for highly-mobile millimeter wave systems," *IEEE Access*, vol. 6, pp. 37 328–37 348, 2018.
- [14] V. Va, T. Shimizu, G. Bansal, and R. W. Heath, "Online learning for position-aided millimeter wave beam training," *IEEE Access*, vol. 7, pp. 30 507–30 526, 2019.
- [15] M. Hussain and N. Michelusi, "Second-best beam-alignment via bayesian multi-armed bandits," in *2019 IEEE Globecom*, 2019, to appear. [Online]. Available: <http://arxiv.org/abs/1906.04782>
- [16] S. Chiu, N. Ronquillo, and T. Javidi, "Active learning and csi acquisition for mmwave initial alignment," *IEEE Journal on Selected Areas in Communications*, pp. 1–1, 2019.
- [17] M. Hussain and N. Michelusi, "Energy-efficient interactive beam alignment for millimeter-wave networks," *IEEE Transactions on Wireless Communications*, vol. 18, no. 2, pp. 838–851, Feb 2019.
- [18] T. Camp, J. Boleng, and V. Davies, "A survey of mobility models for ad hoc network research," *Wireless communications and mobile computing*, vol. 2, no. 5, pp. 483–502, 2002.
- [19] R. R. Roy, *Random Gauss–Markov Mobility*. Boston, MA: Springer US, 2011, pp. 311–344. [Online]. Available: https://doi.org/10.1007/978-1-4419-6050-4_10
- [20] T. Bai and R. W. Heath, "Coverage analysis for millimeter wave cellular networks with blockage effects," in *2013 IEEE Global Conference on Signal and Information Processing*, Dec 2013, pp. 727–730.
- [21] N. Michelusi, U. Mitra, A. F. Molisch, and M. Zorzi, "Uwb sparse/diffuse channels, part i: Channel models and bayesian estimators," *IEEE Transactions on Signal Processing*, vol. 60, no. 10, pp. 5307–5319, Oct 2012.
- [22] S. Noh, M. D. Zoltowski, and D. J. Love, "Multi-Resolution Codebook and Adaptive Beamforming Sequence Design for Millimeter Wave Beam Alignment," *IEEE Transactions on Wireless Communications*, vol. 16, no. 9, pp. 5689–5701, Sep. 2017.
- [23] J. D. C. Little and S. Graves, *Little's Law*, 07 2008, pp. 81–100.
- [24] J. Pineau, G. Gordon, and S. Thrun, "Anytime point-based approximations for large pomdps," *J. Artif. Int. Res.*, vol. 27, no. 1, pp. 335–380, Nov. 2006.
- [25] S. P. Boyd and L. Vandenberghe, *Convex optimization*. Cambridge Univ. Pr., 2011.